

IF GOINGTOCRASH(): DONT()

# RISC-V ARCHITECTURE FOR MOTION PLANNING ALGORITHMS IN AUTONOMOUS UAVS

A senior design project submitted in partial fulfillment of the requirements for the degree of  
Bachelor of Science at Harvard University

Anthony J.W. Kenny  
S.B. Candidate in Electrical Engineering

Faculty Advisor: Vijay Janapa Reddi

Harvard University School of Engineering and Applied Sciences  
Cambridge, MA

March 1st, 2020  
Version: 4.2

Fix Cover Page Formatting

## **Abstract**

This thesis describes a process for accelerating motion planning in autonomous robots through the design of specialised microarchitecture and instruction set architecture. First, it shows the analysis of computational performance of Rapidly-exploring Random Tree (RRT), a sampling-based motion planning algorithm commonly used in autonomous drones. Having identified collision detection as the biggest area of opportunity for improved performance, it describes the process of designing specialized hardware, taking advantage of parallelization, that quickly detects collisions. Finally, it presents how this specialized functional unit can be implemented in a processor, and a RISC-V Instruction Set Architecture (ISA) extension designed to massively reduce the execution time of collision detection.

Rewrite Abstract

# Contents

<b>Preface</b>	<b>i</b>
Abstract . . . . .	i
Table of Contents . . . . .	ii
List of Acronyms . . . . .	v
List of Algorithms . . . . .	vii
List of Figures . . . . .	viii
List of Tables . . . . .	ix
<b>1 Introduction</b>	<b>1</b>
1.1 Problem Summary . . . . .	1
1.1.1 Background . . . . .	1
1.1.2 Problem Definition . . . . .	4
1.2 Prior Work . . . . .	4
1.2.1 Hardware Acceleration . . . . .	4
1.2.2 RISC-V . . . . .	6
1.3 Project Overview . . . . .	8
1.3.1 Proposed Solution . . . . .	8
1.3.2 Project Specifications . . . . .	9
1.3.3 Project Structure . . . . .	9
<b>2 Motion Planning in Software</b>	<b>11</b>
2.1 Motion Planning Background . . . . .	11
2.1.1 Key Concepts . . . . .	12
2.1.2 Rapidly-exploring Random Tree . . . . .	14
2.2 Implementation of RRT . . . . .	18
2.2.1 Technical Specifications . . . . .	18
2.2.2 Implementation Design . . . . .	19
2.2.3 Implementation Visualization . . . . .	20
2.3 Analysis of RRT . . . . .	23
2.3.1 Experimental Methodology . . . . .	23

2.3.2 Results . . . . .	24
<b>3 Motion Planning in Hardware</b>	<b>28</b>
3.1 Defining the Collision Detection Unit . . . . .	28
3.1.1 Edge Collision Function . . . . .	28
3.1.2 Technical Specifications . . . . .	30
3.2 HoneyBee . . . . .	32
3.2.1 HoneyBee Interface Design . . . . .	33
3.2.2 HoneyBee Implementation . . . . .	35
3.2.3 HoneyBee Acceleration . . . . .	39
<b>4 RISC-V Processor</b>	<b>45</b>
4.1 Introduction to the Reduced Instruction Set Computer . . . . .	45
4.1.1 Instruction Set Architecture . . . . .	45
4.1.2 RISC Processor Design . . . . .	45
4.2 RISC-V ISA . . . . .	46
4.2.1 RV32I . . . . .	46
4.2.2 Motion Planning Extension . . . . .	47
4.3 PhilosophyV . . . . .	47
4.3.1 Baseline Implementation . . . . .	47
4.3.2 Implementing HoneyBee . . . . .	49
4.4 Performance Analysis . . . . .	49
<b>5 Conclusion</b>	<b>50</b>
5.1 Discussion of Results . . . . .	50
5.2 Evaluation of Success . . . . .	50
5.3 Future Work . . . . .	50
<b>Bibliography</b>	<b>51</b>
<b>Glossary</b>	<b>53</b>
<b>Appendices</b>	<b>56</b>
<b>A Project Repository</b>	<b>57</b>
<b>B Budget</b>	<b>58</b>
<b>C RRT Supporting Documentation</b>	<b>59</b>
C.1 Justification of Modelling UAV as Prism . . . . .	59
C.2 Full Technical Specifications for RRT Implementation . . . . .	60
C.3 Assessment of Existing RRT Implementations . . . . .	61

C.4	Implementation of Key RRT Functions . . . . .	62
C.5	Geometrically Determining Segment-Plane Intersection . . . . .	65
C.6	Timing Methodology of RRT Analysis . . . . .	66
<b>D</b>	<b>HoneyBee Supporting Documentation</b>	<b>68</b>
D.1	Full Technical Specifications for Edge Collision Detection Unit . . . . .	69
D.2	IEEE Standard for Floating-Point Arithmetic . . . . .	70
D.3	Mapping HoneyBee's Output Sequence to a Grid-Map . . . . .	70
D.4	HoneyBee Handshake Control Protocol . . . . .	71
D.5	HoneyBee Interface Synthesis Report . . . . .	72
D.6	HoneyBee Timing Reports . . . . .	72
D.7	HoneyBee-B Variants . . . . .	72

## List of Acronyms

**2D** 2-Dimensional

**3D** 3-Dimensional

**API** Application Programming Interface

**ARM** Advanced RISC Machine

**ASP** Application Specific Processor

**CISC** Complex Instruction Set Computer

**CPI** Cycles Per Instruction

**CPU** Central Processing Unit

**CSV** Comma Separated File

**DOF** Degree-of-Freedom

**FPGA** Field Programmable Gate Array

**GPU** Graphics Processing Unit

**HB-A** HoneyBee-A

**HB-B** HoneyBee-B

**HB-C** HoneyBee-C

**HDL** Hardware Description Language

**HLS** High Level Synthesis

**IEEE754** IEEE Standard for Floating-Point Arithmetic

**ISA** Instruction Set Architecture

**LUT** Look-Up Table

**OGM** Occupancy Grid Map

**PRM** Probabilistic Road Map

**RISC** Reduced Instruction Set Computer

**RRT** Rapidly-exploring Random Tree

**RRT\*** Rapidly-exploring Random Tree Star

**RTOS** Real-Time Operating Systems

**RV32I** RISC-V 32-Bit Integer

**SoC** System on Chip

**UAV** Unmanned Aerial Vehicle

## List of Algorithms

2.1	Rapidly-Exploring Random Tree in Free Configuration Space . . . . .	15
2.2	Rapidly-Exploring Random Tree with Collision Detection . . . . .	17
C.1	getRandomConfig() as implemented for RRT . . . . .	62
C.2	findNearestConfig() as implemented for RRT . . . . .	62
C.3	stepFromNearest() as implemented for RRT . . . . .	63
C.4	configCollision() as implemented for RRT . . . . .	63
C.5	configCollision() as implemented for RRT for 3D . . . . .	64

## List of Figures

1.1	Simple Visualization of Computer Implementation Hierarchy . . . . .	5
1.2	Typical Process of Adding Non-Standard Extension to RISC-V ISA . . . . .	7
1.3	System Diagram of Overall Project . . . . .	8
2.1	Example of 2 Robot Configurations in 3D Space for Motion Planning Purposes	13
2.2	Occupancy Grid Maps for a $(16 \times 16)$ Workspace of Different Resolutions . .	14
2.3	Scope of the RRT Algorithm . . . . .	15
2.4	Demonstration of RRT Algorithm for 2D robot in 2D space. . . . .	16
2.5	Demonstration of the 5 Key Functions that Constitute RRT . . . . .	20
2.6	Visualization of Workspace in 2D and 3D . . . . .	21
2.7	Visualization of Obstacles in 2D and 3D . . . . .	22
2.8	Complete Visualization of RRT in 2D and 3D . . . . .	22
2.9	Increasing Total Execution Time of RRT with Map Size . . . . .	25
2.10	Profile of Computational Load of RRT in 2D . . . . .	26
2.11	Profile of Computational Load of RRT in 3D . . . . .	27
3.1	Detecting Grid Intersections by Finding Intersections with Axis Oriented Planes . . . . .	29
3.2	Edge Collision Computation Process . . . . .	30
3.3	Megalong Park Honey Bee Pollinating a Weeping Cherry Blossom . . . . .	32
3.4	. . . . .	33
3.5	General Overview of HoneyBee Interface . . . . .	33
3.6	Port Diagram of HoneyBee Interface . . . . .	34
3.7	The Impact of $\epsilon$ on the Length of the Bit-Collision Sequence . . . . .	35
3.8	The Harvard Mark I Computer . . . . .	36
3.9	The Hardware Development Process . . . . .	36
3.10	Hardware Optimization Process . . . . .	38
3.11	HB-A Performance Against Benchmark CPU . . . . .	39
3.12	Timing Diagrams Showing Parallelization in HoneyBee-B . . . . .	40
3.13	HB-B Performance Against Benchmark CPU . . . . .	42
3.14	Timing Diagrams Showing Parallelization in HoneyBee-C . . . . .	43
4.1	5-Stage Reduced Instruction Set Computer (RISC) Datapath . . . . .	45
4.2	Philosophy V Processor . . . . .	48
C.1	Modelling a UAV as a Rectangular Prism . . . . .	59
C.2	Using Parallel Planes to determine Edge Collisions with Grids . . . . .	65

## List of Tables

1.1	List of System Components and their Descriptions . . . . .	9
2.1	Abbreviated Technical Specifications for RRT Implementation . . . . .	18
2.2	RRT Implementation Parameters . . . . .	19
2.3	Optimal RRT Parameters for each Map Size . . . . .	24
3.1	Performance Specifications for Edge Collision Detection Unit . . . . .	30
3.2	Interface Specifications for Edge Collision Detection Unit . . . . .	31
3.3	Synthesis Results for HB-A with $\epsilon = 4$ . . . . .	37
3.4	Synthesis Results for HB-B3 with $\epsilon = 4$ . . . . .	41
3.5	Synthesis Results for HB-C with $\epsilon = 4$ . . . . .	44
4.1	Register State for RV32I Base Instruction Set . . . . .	46
4.2	RV32I Base Instruction Formats . . . . .	47
C.1	General Technical Specifications for RRT Implementation . . . . .	60
C.2	Required Parameters for RRT Implementation . . . . .	61
C.3	Evaluation of Existing Open-Source Implementations of RRT . . . . .	61
C.4	Comparison of Timing Methods . . . . .	67
D.1	Full Technical Specifications for Edge Collision Detection Unit . . . . .	69
D.2	Description of the ports associated with the handshake protocol for HoneyBee	71
D.3	HoneyBee Interface Synthesis Report . . . . .	72

# Chapter 1

## Introduction

Define goal: Somewhere here I need to define very clearly the following

1. Overall Goal: ~ Deliver an example of how RISC-V can be leveraged to design a custom processor for motion planning
2. 4 Objectives:
  - Profile a standard motion planning algorithm to determine the bottleneck function
  - Design a functional hardware unit that eliminates that bottleneck
  - Define a non standard extension
  - Implement Processor and verify all above

### 1.1 Problem Summary

#### 1.1.1 Background

The Unmanned Aerial Vehicle (UAV) has been utilised in military applications extensively throughout the late 20th and early 21st century. However, over the last decade, their use in non-military applications, such as commercial, scientific, agricultural, and recreational, has increased such that the number of civilian drones vastly outnumber military UAVs. Particularly in the commercial sector, such rapid growth in the number and range of applications means that autonomy is key for the profitable adoption of UAVs. Such autonomy relies on efficient computation of motion planning algorithms. However, the implementation of these algorithms can be quite computationally expensive, and thus slow and/or detrimentally power consuming. As such, this thesis aims to design specialized hardware to more efficiently compute motion plans for autonomous drones.

cite

## Autonomous Robotics

For well over 2000 years, the concept of robotics, albeit not always with such a term, has fascinated humans. As early as the first century A.D., the Greek mathematician and engineer, Heron of Alexandria, described more than 100 different machines and automata in *Pneumatica* and *Automata* [1]. In 1898, Nikola Tesla demonstrated the first radio-controlled vessel. Since then, the world has seen widespread application of robotics in manufacturing, mining, transport, exploration, and weaponry. For the last few decades, robots have operated in controlled, largely unchanging environments (e.g. an assembly line) where their environment and movements are largely known *a priori*.

However, in recent years a new generation of autonomous robots has been developed for a wide range complex applications. These new robots are required to adapt to the changing environments in which they operate; most often, this means planning their own paths through space. As such, they must perform motion planning in real-time.

## Motion Planning

While most creatures in the animal kingdom find it relatively easy to navigate their surroundings, autonomous robots must be taught explicitly how to do so by their programmers. Motion Planning refers to the problem of algorithmically determining a collision-free path between two points in an obstacle-ridden space. Chapter 2 provides a detailed explanation of motion planning and of Rapidly-exploring Random Tree (RRT), a commonly used motion planning algorithm.

On the algorithmic and software level, motion planning has been extensively studied and optimized. Even so, current software implementations running on regular Central Processing Units(CPUs) are too slow to execute in real-time for robots to operate in rapidly changing, high complexity environments. More powerful, highly parallelized Graphics Processing Units(GPUs) can be used in tethered robot applications (e.g. robotic arms autonomously executing pick-and-place functions). However, such GPUs consume far too much power to be used in autonomous drones, which are untethered and must sustain flight for useful periods of time. (A typical CPU uses between 65-85 watts, while some GPUs can use up to 270 watts).

cite

## Application Specific Processors

Given the lacking performance in computing motion plans of a CPU, and the untenable power consumption of a GPU, autonomous drone developers are left with the option of developing an Application Specific Processor (ASP), optimized for motion planning.

However, designing a functional, high performance processor from scratch is no small task. It requires expertise in a variety of disciplines (compilers, digital logic, operating systems, etc), and an extraordinary amount of time and effort to develop and verify before it can be used. In short, it's an expensive process, which is why the market for computer

processors is dominated by companies like Intel, AMD, and ARM. The sharing of processor designs is also not possible, as commercial designs are proprietary and competing designs are not encouraged.

Finally, even if one were to design an ASP from scratch, or build off an existing commercial design (which means paying royalties), the Instruction Set Architecture (ISA) that the processor implements are not designed for are not designed for extendability, meaning that even a highly specialized processor is limited to a small number of instructions.

Discuss Moore's law and denard scaling

## RISC-V

RISC-V (pronounced “risk-five”) is an ISA developed by the University of California, Berkeley. It is established on the principles of a RISC, a class of instruction sets that allow a processor to have fewer Cycles Per Instruction (CPI) than a Complex Instruction Set Computer (CISC) (x86, the ISA on which macOS and linux operating systems run, is an example of a CISC instruction set).

What makes RISC-V unique is its open-source nature. RISC-V was started with the philosophy of creating a practical, open-source ISA that was usable in any hardware or software without royalites. The first report describing the RISC-V Instruction Set was published in 2011 by Andrew Waterman, Yunsup Lee, David A. Patterson, and Krste Asanović [2].

### 1.1.2 Problem Definition

#### Problem Statement

Motion planning algorithms implemented in software that runs on general purpose CPUs cannot execute quickly enough for fully autonomous UAVs to operate in high-complexity environments. The state-of-the-art strategy of using power-hungry GPUs to accelerate the execution of these algorithms requires too much power to be cost-effective or feasible for UAVs to sustain flight for useful periods of time.

Improve Problem Statement: Existing research into accelerating robotic motion planning is <reason for RISC-V, inaccessible?> and mainly focussed on tethered arm moving robots.

#### End User

This thesis aims to provide developers of autonomous drones with specialized hardware for motion planning. Such developers have a need for computing hardware that executes motion planning algorithms faster and more power efficiently than existing methods. This thesis will provide a processor design that is synthesizable on an Field Programmable Gate Array (FPGA), giving developers a processor for which a Real-Time Operating Systems (RTOS), or bare metal code, can be deployed.

Revise End User

## 1.2 Prior Work

### 1.2.1 Hardware Acceleration

Hardware acceleration refers to the strategy of using computer hardware specifically designed to execute a function more efficiently than can be achieved by software running on a general purpose CPU. Specialized hardware designed to perform specific functions can yield significantly higher performance than software running on general purpose processors, and lower power consumption than GPUs.

#### Computer Implementation Hierarchy

To briefly frame the space in which this thesis operates, consider the typical computer implementation hierarchy, demonstrated in Figure 1.1. **User level applications**, such as Google Chrome, Microsoft Word, and Apple's iTunes, sit at the top of the abstraction hierarchy. These applications are implemented in **High-Mid Level Languages**, such as C/C++, Python, Java, etc. These programming languages have their own hierarchy, but for the purpose of this thesis, it is sufficient to understand that these programming languages are then compiled into **Assembly Language**. Assembly language closely follows the execution of instructions on the **processor**, and is defined by an **ISA**. An ISA can be

thought of as the contract between software programmers and processor engineers, agreeing what instructions the processor is able to implement. This assembly code is finally loaded into the processor's instruction memory and executed.

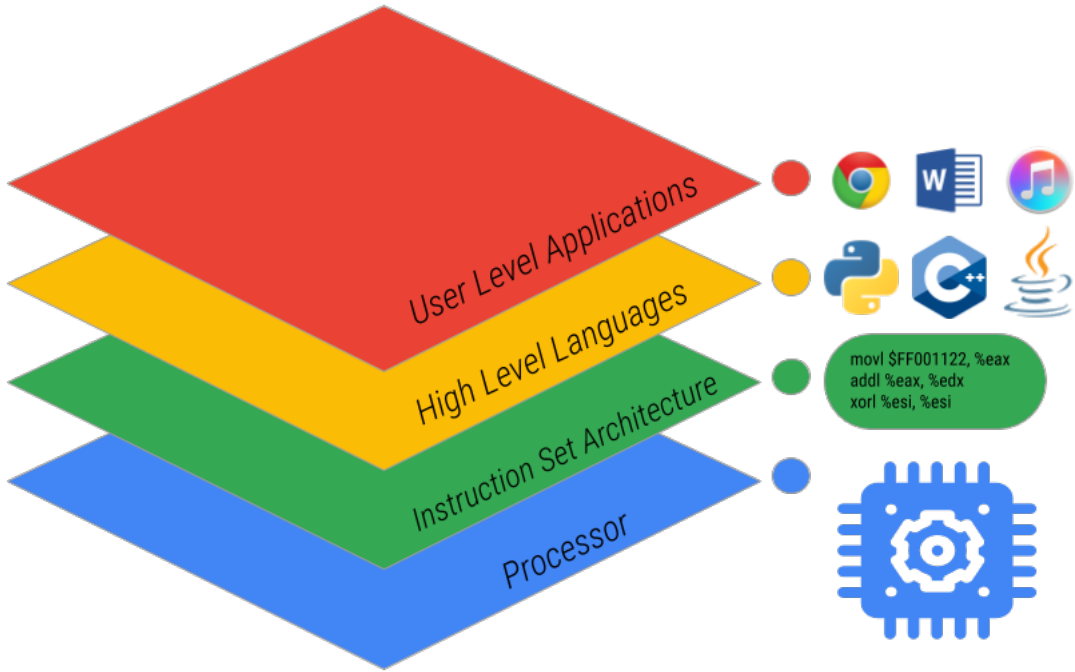


Figure 1.1: Simple Visualization of Computer Implementation Hierarchy

As will be outlined in Section 1.3, this thesis operates extensively on the lower two levels of this hierarchy, extending an existing ISA and building hardware at the processor level that supports these extensions.

### Acceleration of Motion Planning

Accelerating motion planning with hardware is a fairly well studied problem.

*A Motion Planning Processor on Reconfigurable Hardware* [3] studied the performance benefits of using FPGA-based motion planning hardware as either a motion planning processor, co-processor, or collision detection chip. It targeted the feasibility checks of motion planning (largely collision detection) and found their solution could build a roadmap using the Probabalistic Road Map (PRM) algorithm up to 25 times faster than a Pentium-4 3Ghz CPU could.

In *A Programmable Architecture for Robot Motion Planning Acceleration* [4], Murray et

al. built on the work of the aforementioned paper, to accelerate several aspects of motion planning in an efficient manner.

*FPGA based Combinatorial Architecture for Parallelizing RRT* [5] studies the possibility of building architecture to allow multiple RRTs to work simultaneously to uniformly explore a map. Taking advantage of hardware parallelism allows systems such as this to compute more information per clock cycle.

Finally, in the paper *Robot Motion Planning on a Chip* [6], Murray et al. describe a method for constructing robot-specific hardware for motion planning, based on the method of constructing collision detection circuits for PRM that are completely parallelised, such that edge collision computation performance is independent of the number of edges in the graph. With this method, they could compute motion plans for a 6-degree-of-freedom robot more than 3 orders of magnitude faster than previous methods.

### 1.2.2 RISC-V

#### Extending RISC-V

RISC-V is designed cleverly in a modular way, with a set of base instruction sets and a set of standard extensions. As a result, processors can be designed to only implement the instruction groups it requires, saving time, space and power on instructions that won't be used. In addition, another goal of RISC-V is to provide a basis for more specialized instruction-set extensions or more customized accelerators. This is described in the most recent *RISC-V Instruction Set Manual* [7]. This is a powerful feature, as it does not break any software compatibility, but allows for designers to easily follow the steps outlined in Figure 1.2. From a hardware acceleration point of view, this is particularly useful as it allows the designer to directly invoke whatever functional unit or accelerator they implement from assembly code.

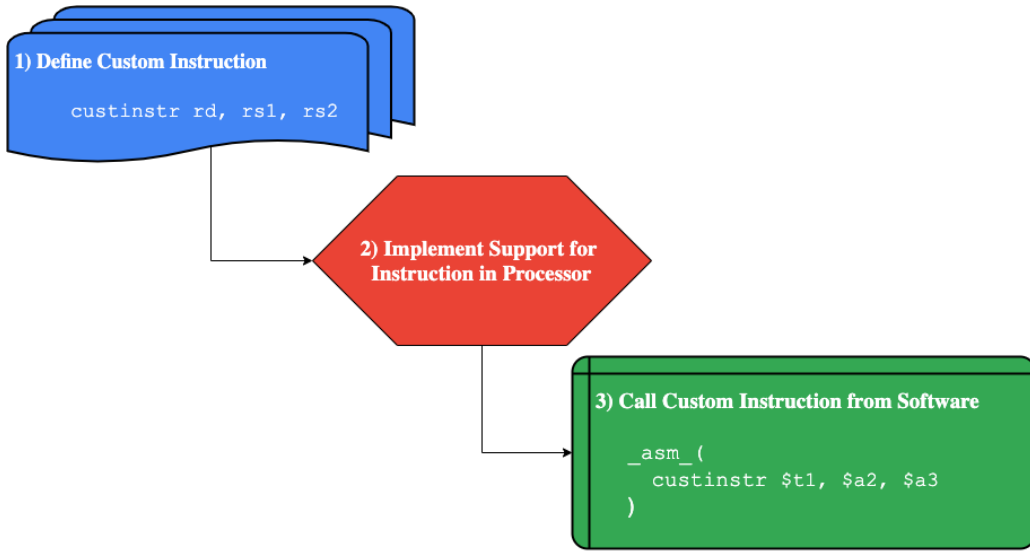


Figure 1.2: Typical Process of Adding Non-Standard Extension to RISC-V ISA

### Accelerating RISC-V Processors

Having only been released in 2011, RISC-V is still a relatively unexplored opportunity for non-education applications. However, it shows promise in the commercial space, with Alibaba recently developing the Xuantie, a 16-core, 2.5GHz processor, currently the fastest RISC-V processor. Recently there has been promising research into accelerating computationally complex applications, particularly in edge-computing, with RISC-V architecture. *Towards Deep Learning using TensorFlow Lite on RISC-V*, a paper co-written by the faculty advisor of this thesis, V.J. Reddi, presented the software infrastructure for optimizing the execution of neural network calculations by extending the RISC-V ISA and adding processor support for such extensions. A small number of instruction extensions achieved coverage over a wide variety of speech and vision application deep neural networks. Reddi et al. were able to achieve an 8 times speedup over a baseline implementation when using the extended instruction set. *GAP-8: A RISC-V SoC for AI at the Edge of the IoT* proposed a programmable RISC-V computing engine with 8-core and convolutional neural network accelerator for power efficient, battery operated, IoT edge-device computing with order-of-magnitude performance improvements with greater energy efficiency.

## 1.3 Project Overview

### 1.3.1 Proposed Solution

This thesis proposes a non-standard RISC-V Instruction Set Extension, supported by a functional unit embedded in a FPGA synthesizable processor design that more rapidly computes motion planning for autonomous UAVs. It will use the RRT algorithm as a benchmark for performance analysis. Profiling of RRT described in chapter 2 found that edge collision detection was the most performance limiting function of RRT. As such, this thesis aims to design a RISC-V extension and specific circuitry that support the faster execution of edge collision detection.

### System Overview

Figure 1.3 shows a high level overview of the system this thesis proposes.

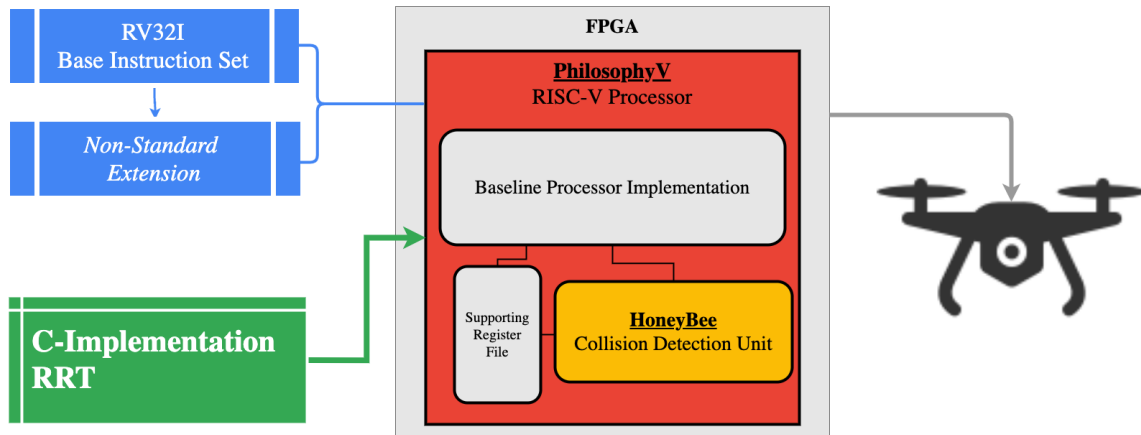


Figure 1.3: System Diagram of Overall Project

The **Extended RISC-V ISA** is made up of the RISC-V 32-Bit Integer (RV32I) Base Instruction Set and a non-standard extension that this thesis will define. The **PhilosophyV Processor** is a RISC-V chip built in Hardware Description Language (HDL) for this thesis. It implements both the RV32I instruction set and the non-standard extension. The PhilosophyV Core includes, along with a baseline 5-stage processor implementation, the **HoneyBee** collision detection unit. A **C Implementation of RRT** is loaded into the instruction memory of the PhilosophyV processor. This processor, synthesized on an **FPGA**, is used as the main processor, co-processor, or accelerator on an **Autonomous UAV**. Table 1.1 outlines the components of this system and their descriptions.

Component	Source	Description
RISC-V Instruction Set		
RV32I	Berkeley	40 Instructions defined such that RV32I is sufficient to form a compiler target and support modern operating systems [7].
Extension	<i>New</i>	This is the custom extension defined by this thesis targeting motion planning instructions. It is outlined in Chapter 4.
C-Implementation of RRT		
RRT	<i>New</i>	Due to lack of available implementations of RRT suitable for the purposes of this thesis, RRT was implemented from the ground up in C. This is detailed in Chapter 2
FPGA Synthesized Chip		
Zynq-7000	Xilinx	The Zynq-7000 family of System on Chip (SoC)s are a low cost FPGA and Advanced RISC Machine (ARM) combined unit.
PhilosophyV	<i>New</i>	The processor built for this thesis to demonstrate how the RISC-V extension and hardware unit work together. This is detailed in Chapter 4
HoneyBee	<i>New</i>	The functional unit designed specifically for faster execution of edge collision detection computations. Outlined in Chapter 3

Table 1.1: List of System Components and their Descriptions

### 1.3.2 Project Specifications

Project Specifications: These need significant revision from the last checkpoint

### 1.3.3 Project Structure

This report is structured to follow the timeline of this project, and is outlined below:

1. A benchmark motion planning algorithm, RRT, was selected and implemented in software. Once implemented, a variety of performance analysis methods were used to profile the computational hotspots of the algorithm. It was found that edge collision detection was the critical function limiting execution time. This process is detailed in Chapter 2.

2. With edge collision detection having been identified as the critical function, the process of designing specialised hardware to execute this function began. The technical specifications, performance specifications, designs, build phases, measurement and analysis of this hardware unit is presented in Chapter 3.
3. With the aforementioned functional unit's performance verified in simulation, the next step was to implement this in a processor. First, a baseline processor was designed and built for this project to implement a base RISC-V instruction set. The performance of RRT is again profiled on this baseline processor (as up until this point, it was profiled on x86 architecture). A non-standard extension to the RISC-V ISA was then defined and support for this was implemented in the processor. Comparative performance analysis was then conducted. This process is described in detail in Chapter 4.
4. Chapter 5 is a discussion of results and future work.

Summary of Results: Do I need a summary of results section in the introduction?

## Chapter 2

# Motion Planning in Software

The first objective of this thesis is to identify a typical motion planning algorithm, profile its execution, and determine computational bottlenecks.

This chapter introduces the concept of motion planning and details the process of implementing and analyzing Rapidly-exploring Random Tree (RRT), a commonly used algorithm, to identify its computational bottlenecks.

Update once I have properly defined goals and objectives

### 2.1 Motion Planning Background

A funny paradox in computer science is the fact that it is relatively easy to teach a computer to perform tasks that humans find very complicated, but extremely difficult to program one to execute functions that humans master during infancy. Consider, it was as early as 1949 that Claude Shannon presented his paper *Programming a Computer for Playing Chess*[8], and by 1997 the *Deep Blue* computer defeated Garry Kasparov, the reigning world champion, in a six game chess match.[9] Compare that with some of the most advanced autonomous humanoid robots to date displaying dexterity only comparable with that of a toddler. The task of finding a collision free path, performed constantly without thought by a human, is an example of this paradigm. For a robot to plan its own paths, it relies on a set of Motion Planning Algorithms.

Motion Planning Algorithms refer to the set of algorithms that find possible sequences of valid configurations for a robot in a space. In more simple terms, they are algorithms that determine the movements a robot can make in a map, with the intent of eventually finding a path from one point to another.

### 2.1.1 Key Concepts

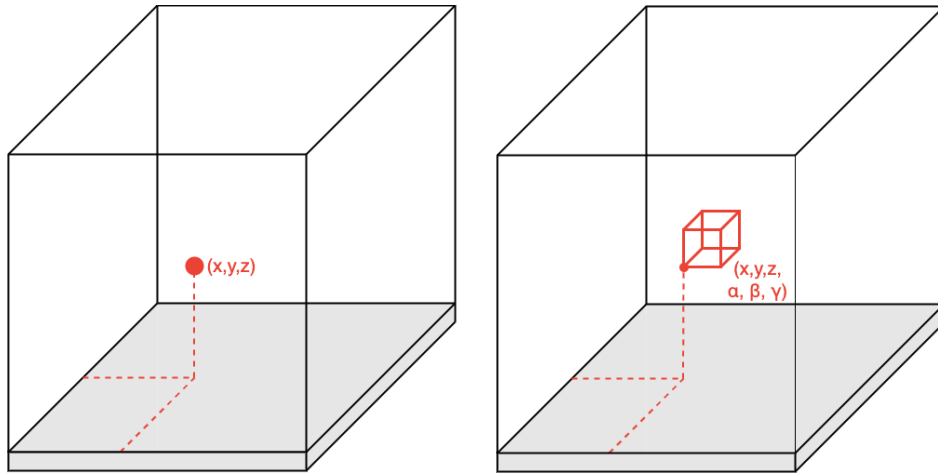
#### Workspace

The workspace, more loosely known as the **map**, is the space which the robot and obstacles occupy. Obviously, **obstacles** refer to anything with which the robot cannot intersect.

#### Configuration

A configuration describes the position, orientation, and pose of the robot. The complexity of a robot's configuration is therefore dependant on the dimension of the workspace, the complexity of the robot itself, and in what level of detail the robot must be represented. For example:

- Most simply, a robot can be represented as a point; by the Cartesian coordinates  $(x, y)$  in 2-Dimensional (2D) space and  $(x, y, z)$  in 3-Dimensional (3D) space.
- More realistically, a robot such as a drone may be represented in 3D as a 3D rectangular prism; by an origin point  $(x, y, z)$  and 3 Euler angles  $(\alpha, \beta, \gamma)$  describing its orientation.
- In a more complex form, a fixed-base,  $N$  Degree-of-Freedom (DOF) robot would require an  $N$ -dimensional configuration.



(a) A robot represented by just a point in 3D space, requiring only 3 Cartesian coordinate  $(x, y, z)$  points to describe its configuration

(b) A robot represented as a cube in 3D space, now requiring 3 Euler angles  $(\alpha, \beta, \gamma)$  along with the original Cartesian coordinates.

Figure 2.1: **Example of 2 Robot Configurations in 3D Space for Motion Planning Purposes**

### Occupancy Grid Map

An Occupancy Grid Map (OGM) is a method of representing the obstacles present in a workspace. Obstacles are often irregularly shaped and computing collisions with such obstacles is near impossible. Therefore, the workspace is discretized into grids, with grids that contain any part of the obstacle marked as occupied, even if only a small part of the grid is occupied. An Occupancy Grid Map (OGM) will more accurately represent a workspace with a higher resolution, shown in Figure 2.2.

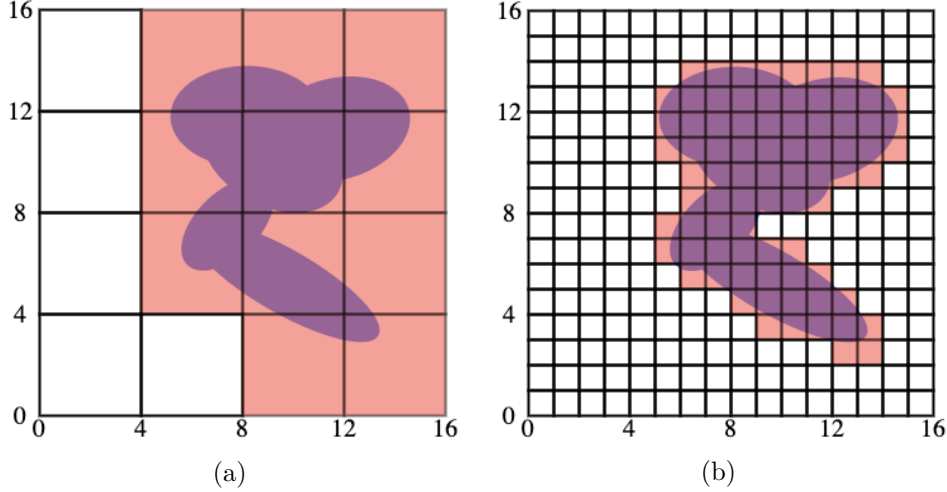


Figure 2.2: **Occupancy Grid Maps for a (16×16) Workspace of Different**

**Resolutions.** Figure 2.2a shows how an OGM with low resolution, while simpler to construct and analyse, will over-represent the obstacle density of a workspace. Figure 2.2b shows how a higher resolution will more accurately reflect the obstacles of a workspace.

### 2.1.2 Rapidly-exploring Random Tree

Rapidly-exploring Random Tree (RRT) is an algorithm designed to efficiently build a tree of collision-free paths in a high-complexity environment. The algorithm grows the tree by randomly sampling points and connecting them to the nearest existing node in the tree. It is inherently biased to grow towards large unsearched areas of the workspace. RRT was developed by S. LaVelle[10] and J. Kuffner[11]. It is frequently used in autonomous robotic motion planning problems such as autonomous drones.

#### Scope

RRT takes an initial configuration, a goal point, and an Occupancy Grid Map (OGM) as its input. This OGM may be built and updated using *a priori* knowledge, sensor data from the robot, and other inputs. The algorithm will output a tree of collision free paths toward the goal, as demonstrated in Figure 2.3. **It does not calculate the fastest path from that tree;** that can be accomplished using algorithms such as Dijkstra's algorithm.

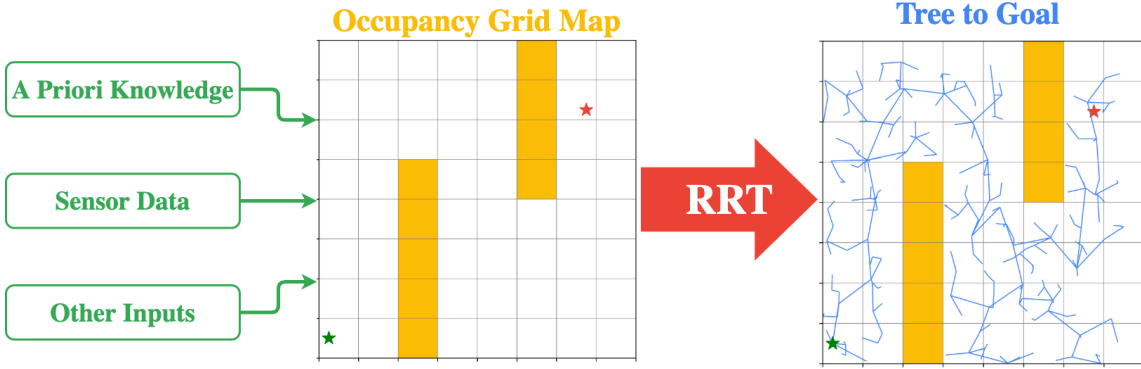


Figure 2.3: **Scope of the RRT Algorithm:** Takes an OGM as input and outputs a tree of collision free paths. The tree is shown in blue on the right.

### Algorithm

Put simply, RRT finds a path from start to finish by randomly exploring a workspace. Put more technically, it builds a tree of possible configurations (also known as a graph), connected by edges, for a robot of some physical description. It does so by selecting random configurations and adding them to the graph. From this graph, a path from the initial configuration to some goal configuration can be found, given a high enough number of iterations. As such, RRT can be considered probabilistically complete. The pseudo-code for RRT can be seen in Algorithm 2.1

---

#### Algorithm 2.1: Rapidly-Exploring Random Tree in Free Configuration Space

---

**Inputs:** Initial configuration  $q_{init}$ ,  
          Number of nodes in graph  $K$ ,  
          Incremental Distance  $\epsilon$

**Output:** RRT Graph  $G$  with  $K$  configurations  $[q]$  & edges  $[e]$

```

G.init() for k = 1 to K do
    qrand ← randomConfiguration()
    qnear ← findNearestConfiguration(qrand, G)
    qnew ← stepFromNearest(qnear, qrand, Δq)
    G.addVertex(qnew)
    G.addEdge(qnear, qnew)
end
  
```

---

Algorithm 2.1 can be visually represented in Figure 2.4, with the example showing a 2D robot operating in a 2D workspace.

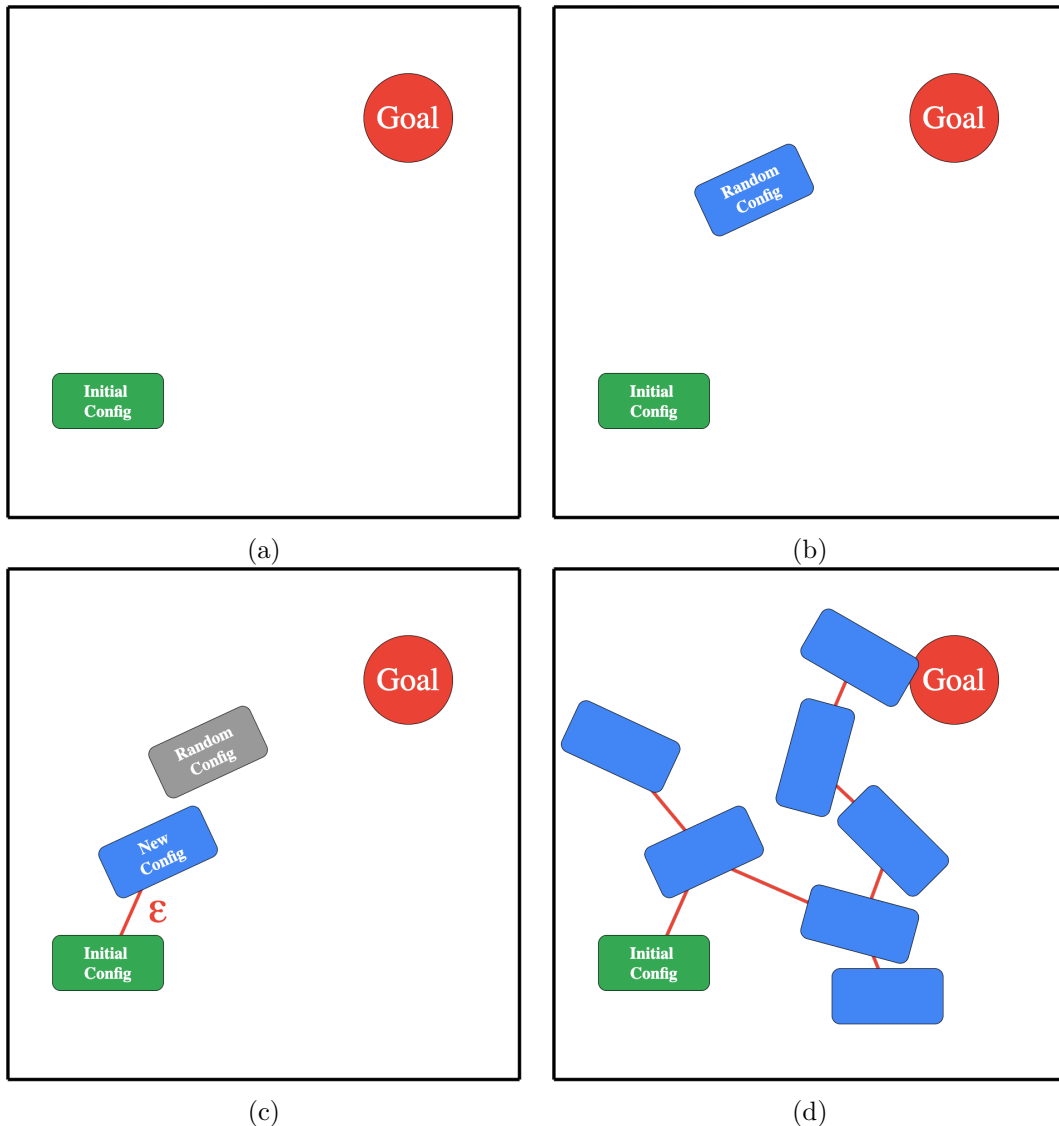


Figure 2.4: **Demonstration of RRT Algorithm for 2D robot in 2D space.** In this example, the graph  $G$  begins with an initial configuration and a goal. In (b), the first random configuration is generated. In this case, the nearest configuration is the initial configuration. The random configuration is more than  $\epsilon$  from the initial configuration, so a new configuration in the direction of the random configuration is generated and added to the graph in (c). This is repeated  $K$  times, until the graph in (d) is generated.

Algorithm 2.1 shows how RRT builds a graph of possible configurations connected

by edges in a completely free configuration space. However, in real-world applications, a robot's workspace space will contain obstacles. As such, collision detection must be included in the algorithm. The two types of collisions the algorithm must check for are *configuration collisions* (those where the robot would collide with an obstacle in a given configuration) and *edge collisions* (where the robot would collide when moving between two collision free configurations).

RRT with configuration and edge collision detection can be seen in Algorithm 2.2. The method of implementing RRT with collision detection to model a drone in 3D space is detailed in Section 2.2.

---

**Algorithm 2.2:** Rapidly-Exploring Random Tree with Collision Detection

---

**Inputs:** Initial configuration  $q_{init}$ ,  
 Number of nodes in graph  $K$ ,  
 Incremental Distance  $\epsilon$ ,  
 Space  $S$  containing obstacles

**Output:** RRT Graph  $G$  with  $K$  configurations  $[q]$  & edges  $[e]$

```

 $G.init();$ 
 $for k = 1$  to  $K$  do
    while !configCollision( $q_{new}$ ) do
         $q_{rand} \leftarrow randomConfiguration();$ 
         $q_{near} \leftarrow findNearestConfig(q_{rand}, G);$ 
         $q_{new} \leftarrow stepFromNearest(q_{near}, q_{rand}, \Delta q);$ 
    end
     $e_{new} \leftarrow newEdge(q_{near}, q_{new})$ 
    if !edgeCollision( $e_{new}$ ) then
         $G.addVertex(q_{new});$ 
         $G.addEdge(q_{near}, q_{new});$ 
    else
        |  $k = k - 1;$ 
    end
end

```

---

## 2.2 Implementation of RRT

### 2.2.1 Technical Specifications

With RRT selected as the benchmark algorithm against which to test specialized hardware, this project required an implementation of the algorithm that satisfied the following criteria shown in Table 2.1. Appendix C.2 is a more thorough description of the technical specifications for the implementation of RRT.

Requirement	Brief Description and Justification
Implemented in C/C++	Implementations in C allow for more accurate analysis of computational bottlenecks, unlike higher-level languages like Python.
3D Workspace	The computational requirements of RRT in 3D differ somewhat to that in 2D. Since autonomous UAVs operate in 3D space, it was necessary to have a 3D implementation to analyse.
UAV modelled as a 3D rectangular prism	In theory, it is possible to model a UAV much more precisely than a rectangular prism. However, in reality, modelling a UAV as a 3D rectangular prism, defined by coordinates $\{x, y, z\}$ and Euler angles $\{\alpha, \beta, \gamma\}$ , is more than sufficient (and more computationally efficient). See Appendix C.1 for justification.
Mathematically Complete Collision Detection	When RRT is implemented for educational purposes, the edge collision calculations are often simplified to a sampling model which is probabilistically complete but not mathematically complete. In other words, it will catch most collisions by sampling a number of points along each edge, but there is always a possibility of an undetected collision. In real world applications, collisions must be calculated by method of geometric intersection to ensure all collisions are detected.
Highly Parameterizable	Accurate analysis of the algorithm required the ability to vary the following parameters: <ul style="list-style-type: none"> <li>• <math>\epsilon</math> (Maximum distance between two configurations)</li> <li>• <math>K</math> (Maximum number of configurations)</li> <li>• <math>DIM</math> (The upper bound of each dimension for a <math>DIM \times DIM \times DIM</math> workspace)</li> <li>• Goal Bias (How biased RRT is to move towards goal point)</li> </ul>

Table 2.1: Abbreviated Technical Specifications for RRT Implementation

The original intention was to find an existing implementation of RRT that could fulfill these requirements. However, no open-source implementations were suitable. Appendix C.3 shows an evaluation of existing implementations.

As a result, it was necessary to build a C implementation of RRT from the ground up to the aforementioned specifications.

### 2.2.2 Implementation Design

The design and implementation of RRT, while necessary, was significant and time consuming. Since this was not the main object of this thesis, only a brief description of key design choices has been included here. Appendix C contains a more detailed account.

System  
Diagram  
Here

#### Parameterization

Table 2.2 shows the parameters that were included in the implementation and compiled by way of a C header file.

Parameter	Data Type	Description
$\epsilon$	Integer	Maximum distance between two configurations
$K$	Integer	Maximum number of configurations in the graph
$DIM$	Integer	Upper bound of each axis of workspace
Goal Bias	Float	Percentage likelihood of stepping towards goal node
OGM	File Pointer	CSV of booleans to represent grids

Table 2.2: RRT Implementation Parameters

#### Dimensionality

RRT was implemented in both 2D and 3D. Not only did a 2D implementation provide a good development checkpoint, it was also interesting to see the difference in computational load between 2D and 3D, shown in Section 2.3.

#### Modelling a UAV

The UAV was modelled as a 3D rectangular prism, with its configuration represented by Cartesian coordinates  $(x, y, z)$  and Euler angles  $(\alpha, \beta, \gamma)$ .

#### Key Functions

Algorithm 2.2 shows that there are 5 key functions that constitute RRT. Figure 2.5 demonstrates each of these functions: `getRandomConfig()`, `findNearestConfig()`, `stepFromNearest()`, `(configCollisions)`, and `edgeCollisions()`. Appendix C.4 shows in detail how each of these functions was implemented.

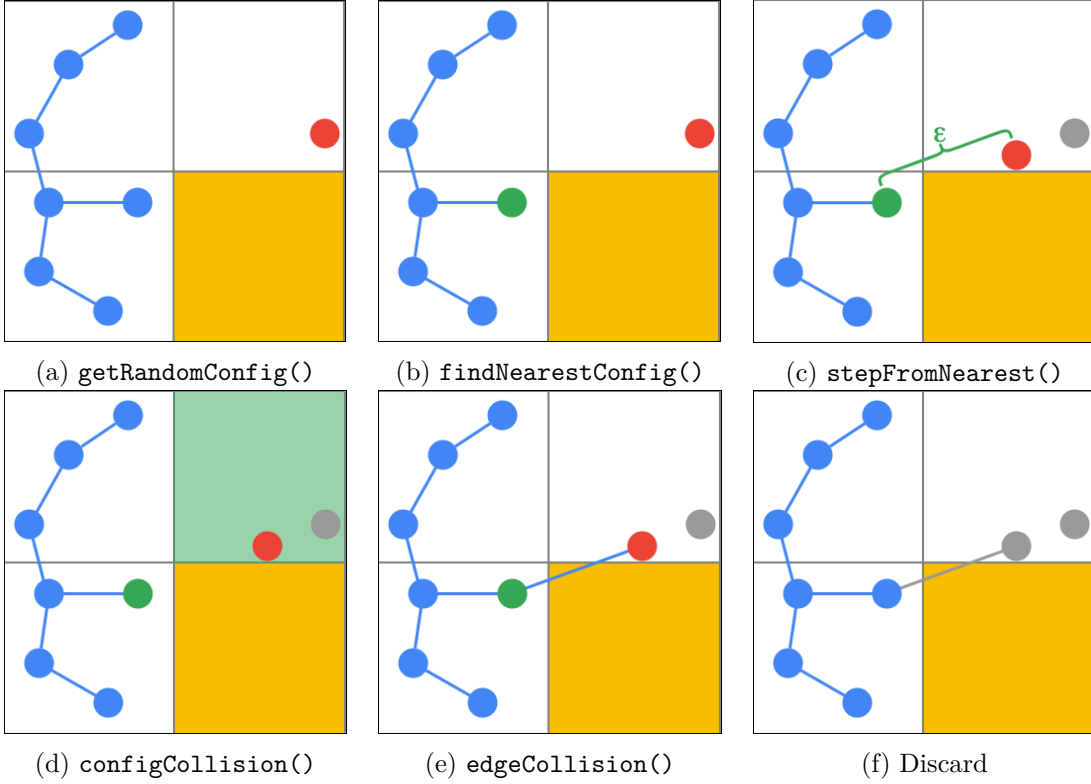


Figure 2.5: **Demonstration of the 5 Key Functions that Constitute RRT**, where configuration is a node in a 2D workspace. A new node is generated in (a) with `getRandomConfig()`, and the closest existing node is found with `findNearestConfig()` in (b). In this case, the new node is further than  $\epsilon$  from the nearest node, and so a new node is generated with `stepFromNearest()` in (c). `configCollision` determines that the new node is not in an occupied grid (d) and draws an edge between the two nodes. `edgeCollision()` determines that, in this case, there is a collision (e) and the new node is discarded (f).

### 2.2.3 Implementation Visualization

With the back end functionality of RRT designed and implemented, it was necessary to develop a way to visualize it. Many existing implementations had the visualization interface run synchronously alongside RRT. This would distort any performance analysis results, and so in this implementation it was left until after RRT had finished executing and then plotted using Python.

### Plotting Configurations and the Workspace

Plotting the workspace using the “matplotlib” library was relatively simple in both 2D and 3D, shown in Figure 2.6. It was decided that the UAV’s configuration would be visualized only as its origin point, rather than plotting a 3D rectangular prism at each configuration, in order to maintain simplicity. Nevertheless, the UAV was still modelled as a 3D prism in the backend.

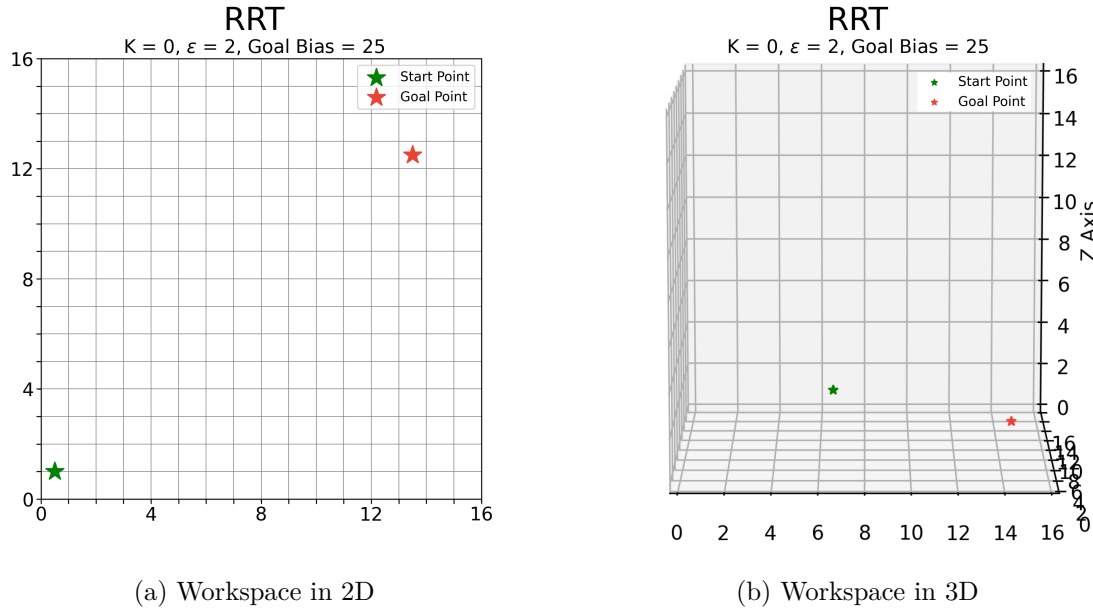


Figure 2.6: **Visualization of Workspace in 2D and 3D**, with configuration represented by only a point, and Start and Goal nodes shown

### Plotting Obstacles

Obstacles were plotted in accordance to the input OGM, shown in Figure 2.7

### Plotting RRT Graph

To keep the plot simple, it was decided to not show the origin point of each configuration in the graph produced by RRT. Instead, only the edges of the graph were plotted, seen in Figure 2.8

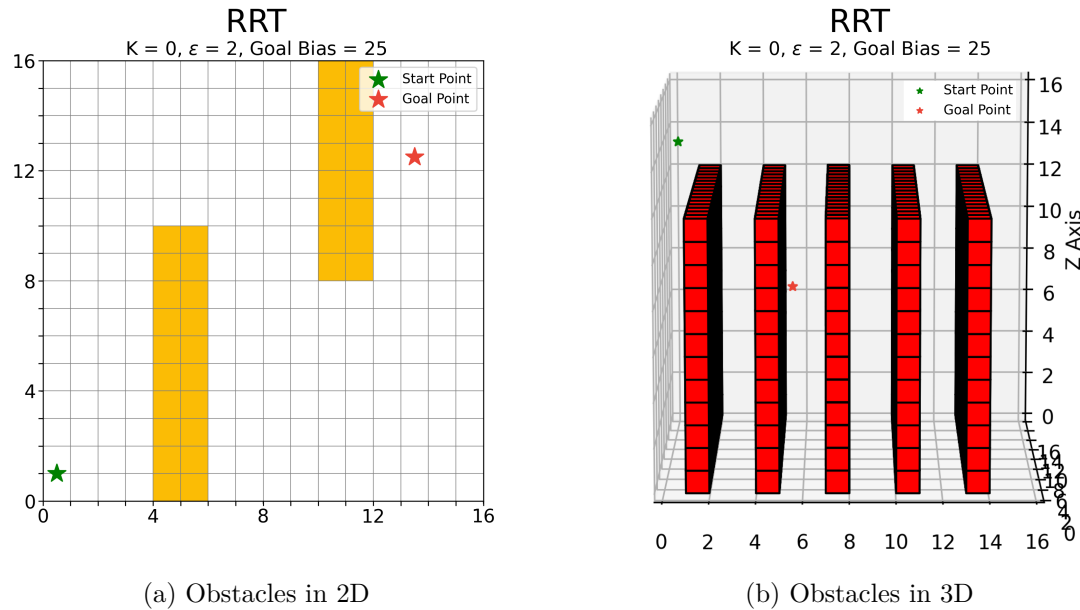


Figure 2.7: **Visualization of Obstacles in 2D and 3D**, Obstacles shown in yellow and red for 2D and 3D respectively.

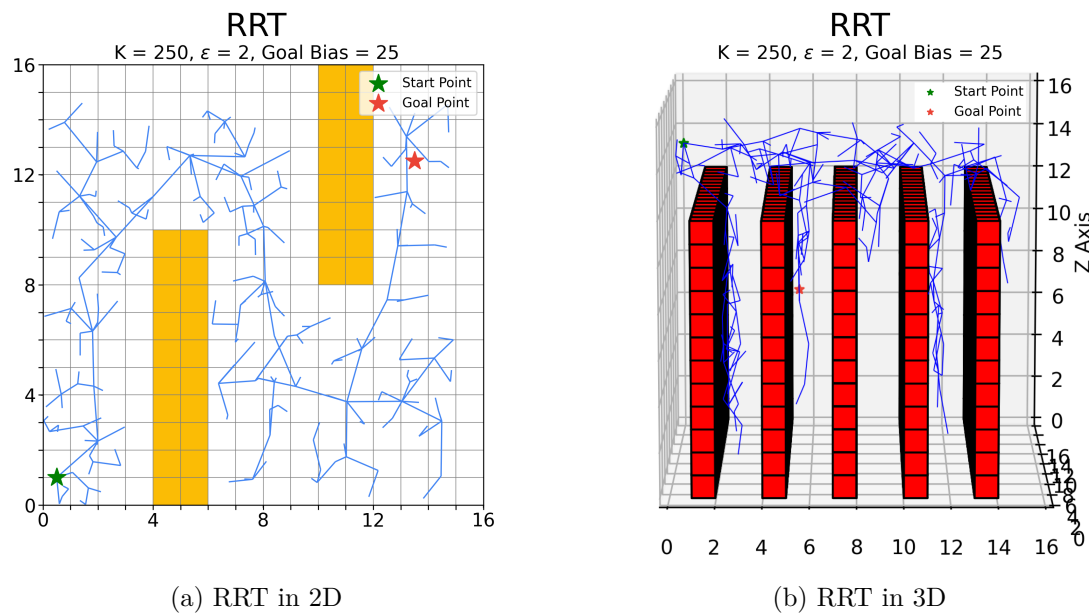


Figure 2.8: **Visualization of Obstacles in 2D and 3D**, with Graph shown in blue.

## 2.3 Analysis of RRT

Having implemented a functioning version of RRT that adhered to the specifications set out in Table 2.1, analysis of its computational profile could begin. The purpose of this analysis was to identify the biggest bottleneck of RRT and therefore the best opportunity for hardware acceleration.

### 2.3.1 Experimental Methodology

Experiments were set up to determine which of the 5 key functions of RRT takes up the biggest share of computational load. The only fair way of determining the computational load of each function was to measure the percentage of CPU time each function takes for the **fastest possible execution** of RRT for a given map size. This is explained in more detail in Section 2.3.1.

#### Measuring Performance

The “performance” metric of interest is the percentage of total time the CPU spends executing each of the 5 key functions. CPU analysis of a program can often be more complicated than merely timing how long each function takes to execute. Software can be written with inbuilt multithreading and other optimizations that require special CPU analysis software, such as Intel’s VTune Profiler[12]. This software is designed to find computational bottlenecks in large, complex programs. However, it takes significantly longer to run (which was unsuitable for running hundreds of thousands of tests), and is less customizable, than adding performance timers directly to the program’s code. It was also hypothesized that, since this project’s implementation of RRT did not use multithreading or any other timing distorting optimizations, custom performance tracking should yield the same results as VTune Profiler. As such, custom performance tracking was added to the RRT implementation. This custom performance tracking method was verified by conducting a  $\chi^2$  test against data from VTune Profiler, and was found to be accurate. Appendix C.6 gives more detail on timing methodology.

#### Optimal Parameters

Extensive testing was undertaken to determine the optimal parameters for a given map size. The goal was to find the set of parameter values for which RRT would reach its goal with  $\geq 98\%$  probability, for a wide variety of OGMs, in the shortest possible time.

For each map size  $\{4, 8, 16, 32, 64\}$ , the parameters that were varied were  $\epsilon$ ,  $K$ , and Goal Bias. The success rate and average execution time was measured by, for each set of parameter values, running RRT 100 times. Thus, with 5 different map sizes, if 4 values were tested for each parameter, and 4 different OGMs were tested, the total number of tests =  $4^4 \times 5 = 1280$  (with each test running RRT 100 times!)

As such, only the optimal parameter values for each map size are included in Table 2.3.

<i>DIM</i>	<i>K</i>	$\epsilon$	Goal Bias (%)	Success Rate (%)
2D				
$4 \times 4$	75	1	10	100
$8 \times 8$	100	2	25	98
$16 \times 16$	125	4	25	99
$32 \times 32$	250	8	10	100
$64 \times 64$	500	16	25	100
3D				
$4 \times 4 \times 4$	75	1	10	99
$8 \times 8 \times 8$	100	2	25	100
$16 \times 16 \times 16$	100	4	25	100
$32 \times 32 \times 32$	250	8	10	99
$64 \times 64 \times 64$	500	16	25	100

Table 2.3: **Optimal RRT Parameters for each Map Size**, shows the optimal set of parameters after extensive testing, alongside their respective success rates over 100 executions of RRT for different OGMS.

### 2.3.2 Results

As expected, the total execution time of RRT for optimal parameters increased with the size of the map, shown in Figure 2.9.

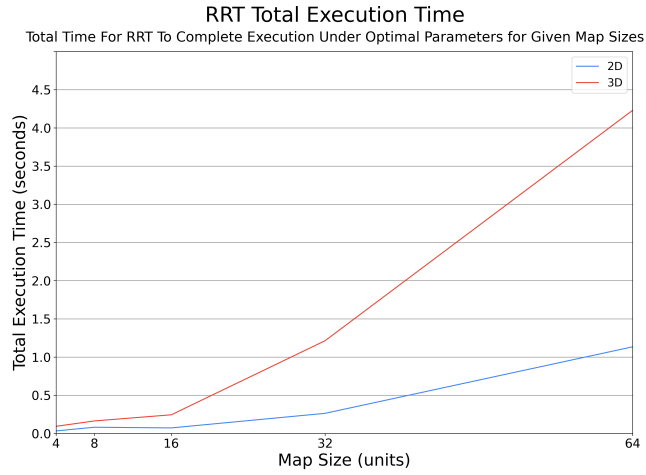


Figure 2.9: Increasing Total Execution Time of RRT with Map Size

## 2D Computational Load Profile

Figure 2.10 shows that the two biggest computational loads are `findNearestConfig()` and `edgeCollisions()`, with the latter increasing as the size of the map increases. The fact that the load of `edgeCollisions()` takes the majority of execution in bigger map sizes means that, at least in 2D, it can be considered the bottleneck function.

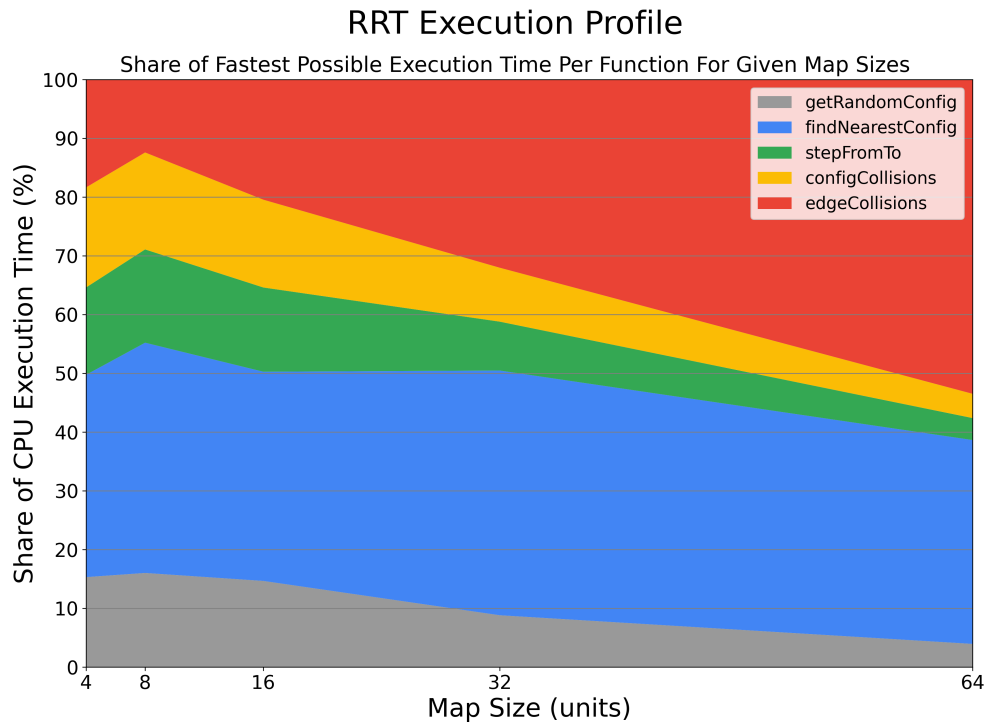


Figure 2.10: **Profile of Computational Load of RRT in 2D**

### 3D Computational Load Profile

The computational load of `edgeCollisions()` was even greater in 3D, starting at 40% for  $4 \times 4 \times 4$  maps and increasing to 70% for  $64 \times 64 \times 64$  maps, as shown in Figure 2.11.

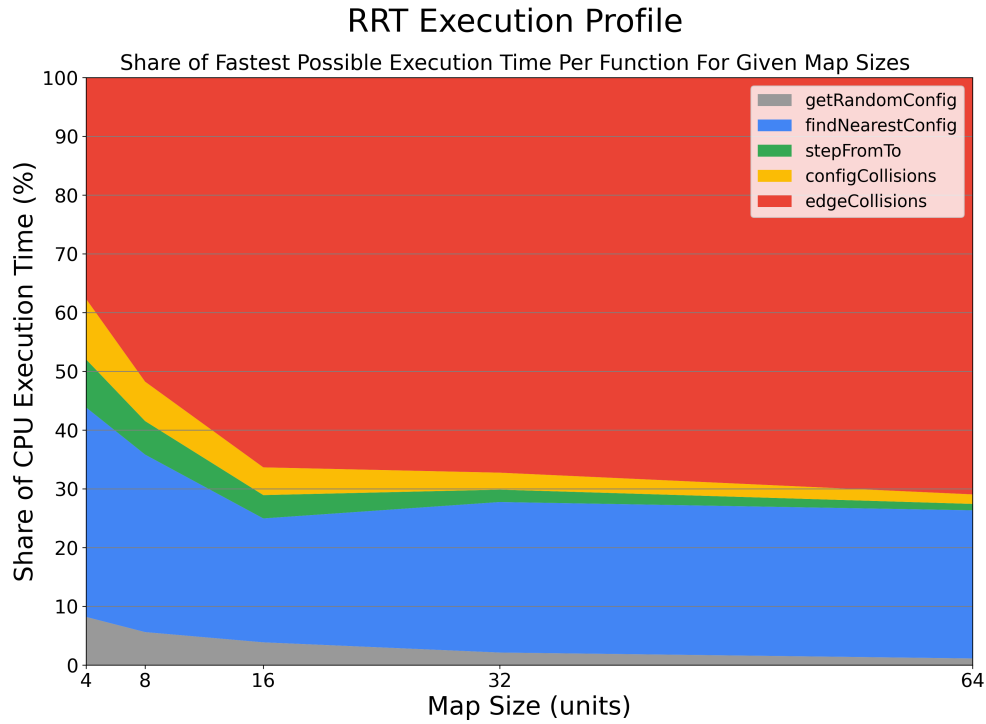


Figure 2.11: **Profile of Computational Load of RRT in 3D**

As such, it is safe to say that the bottleneck function for RRT is `edgeCollisions()`. This conclusion is strengthened by the fact that `edgeCollisions()` was implemented in the fastest possible way (without relying on approximations or implementing multithreading), whereas `findNearestConfig()` was implemented without any optimizations (a possible optimization was the  $K$ -nearest node algorithm, for instance). Finally, this conclusion supports prior research that collision detection takes up the vast majority of CPU execution time. As such, this is the function that was targeted for hardware acceleration.

# Chapter 3

# Motion Planning in Hardware

The second objective of this thesis was to design and implement a functional hardware unit that accelerates the execution of RRT in 3D. With the bottleneck function having been identified in Chapter 2 as edge collision detection, Chapter 3 details the specification, design, implementation, and analysis of a hardware unit that implements the edge collision function.

## 3.1 Defining the Collision Detection Unit

### 3.1.1 Edge Collision Function

To briefly examine the edge collision detection function in general terms; Given an edge  $e$ , RRT finds where  $e$  intersects with grids in the OGM. If any of the grids it intersects with are “occupied”, a collision is returned. This is shown in Figure 3.2 on Page 30.

To see why it is so computationally intense to calculate intersections between a segment and grids, it must be understood that it is a fairly involved geometric process. Figure 3.1 on Page 29 shows how grid intersections are detected by computing the where the segment intersects certain **axis-oriented planes**.

#### Time Complexity

With the steps of the edge collision algorithm understood, (explained graphically in Figure 3.1, algorithm included in Appendix C.4, its Time complexity may be quantified. For an edge  $e$  of maximum length  $\epsilon$ , it must check for intersections with  $\epsilon \times \epsilon \times \epsilon$  grids. (i.e the only grids that are checked are the ones that the  $e$  could possibly intersect with). It first iterates through the three dimensions of axis-oriented planes ( $xy$ ,  $xz$ , and  $yz$ ). This is a constant of 3. Within each of these dimensions, it must iterate through  $\epsilon$  planes. This makes its time complexity  $O(3\epsilon)$ .

Appendix  
Reference?

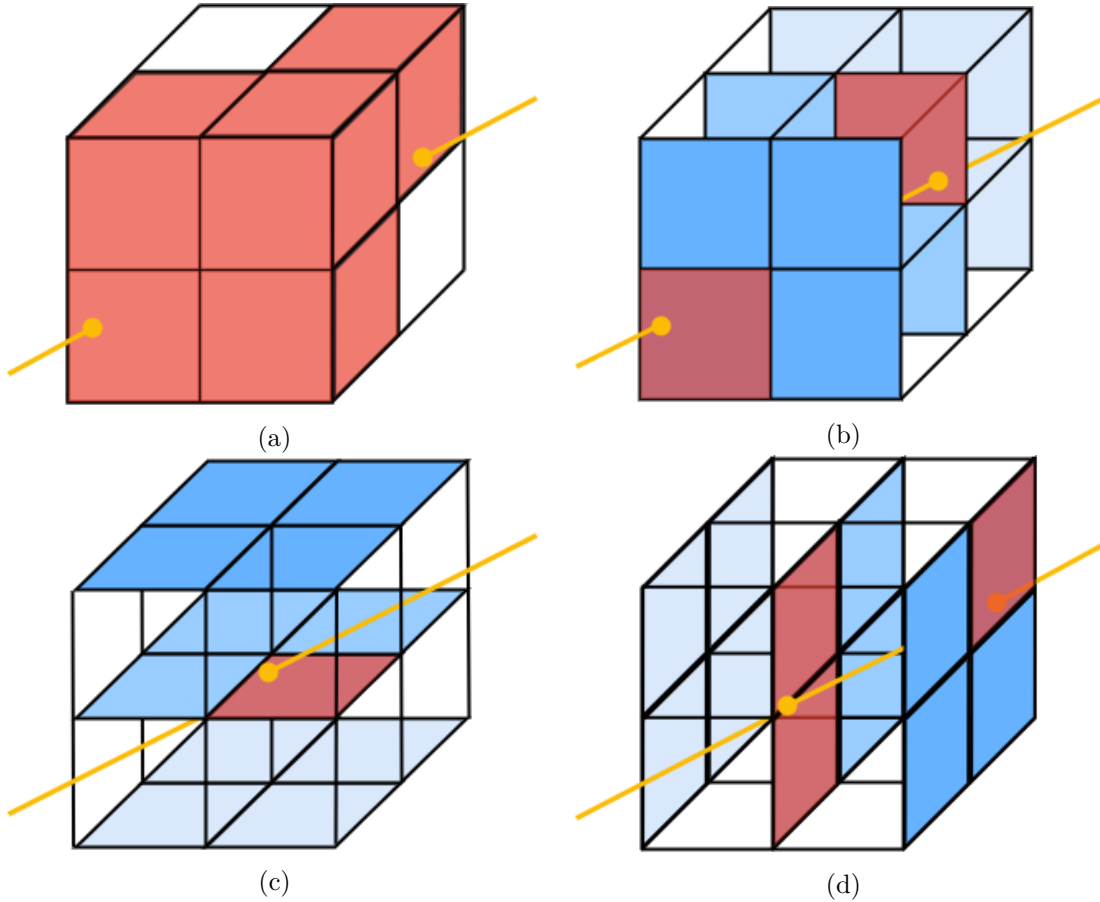


Figure 3.1: **Detecting Grid Intersections by Finding Intersections with Axis Oriented Planes**

Consider an edge  $e$  that spans the width of a  $2 \times 2 \times 2$  grid map, as shown in Figure 3.1 (do not consider if the grids are occupied, this is just to determine which of them the edge intersects). Just by eyeballing Figure 3.1a it seems odd that so many of the grids have been intersected (denoted by red shading) by the yellow edge. The algorithm executed by checking one set of axis-oriented planes at a time. Figure 3.1a shows how the  $xy$ -oriented planes are checked for 3 different values of  $z$  (going into the page), finding two intersection points. There is only one intersection for the  $xz$  oriented planes (3.1c). In Figure 3.1d, the segment intersects 2 grids in the second  $yz$ -oriented plane, and one in the third plane. The intersected grids are thus any grid where a point-of-intersection falls on its face.

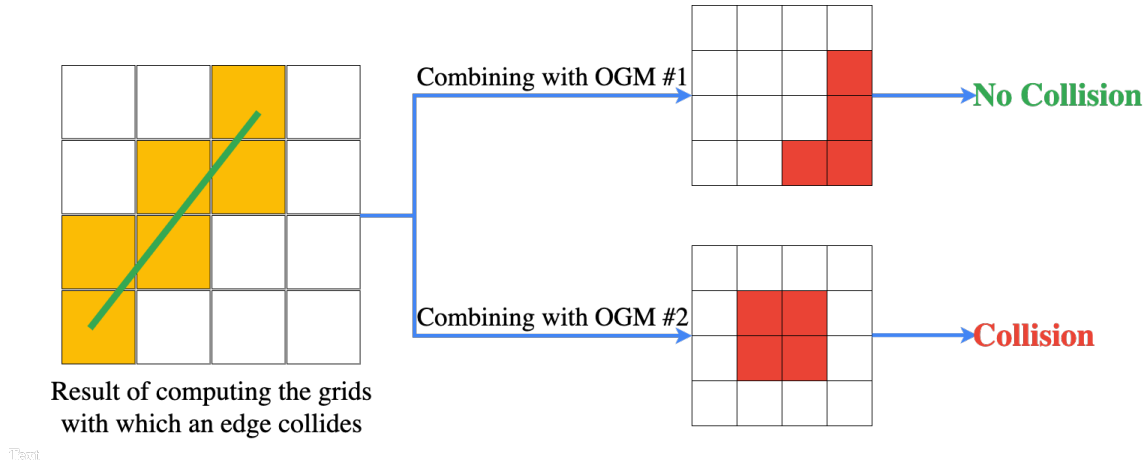


Figure 3.2: **Edge Collision Computation Process.** Most of the computational load is found in determining the grids with which an edge intersects (as seen on the left of the figure). Once these grids have been found, it is very simple (and fast) to lookup if these grids are occupied in the OGM

### 3.1.2 Technical Specifications

#### Performance Specifications

When accelerating motion planning algorithms, it is often difficult to quantify a goal for how much faster one would like the function to run - the answer is usually “as fast as possible!” For this thesis, the performance specification was set to be the edge collision function to run fast enough such that it was no longer the bottleneck function. This translated to a desired speedup of about 3 times (when compared to benchmark performance of a typical CPU). Table 3.1 quantifies this in terms of latency and throughput.

Metric	Benchmark CPU*	Accelerated
Latency ( $\mu$ seconds/edge)	2.6	0.9
Throughput (edges/second)	384,615	1,111,111

Table 3.1: **Performance Specifications for Edge Collision Detection Unit.**

\*Benchmark CPU is an Intel 3.1 GHz i7 Dual Core processor, typical of a laptop computer.

## Area Specifications

Generally, an inverse relationship exists between latency and area. While it may be possible to make the unit much faster than the latency specification, this may become prohibitive with regards to the amount of area on chip it would occupy. It was decided to limit the area to that which would fit on an FPGA typical in drone applications (those of the Kintex-7 Low Voltage family were chosen, but there are many possible options.)

Logic area on an FPGA is largely determined by Look-Up Tables(LUTs). This is a “truth-table” used in FPGAs that determine what output to return for a given input. Any amount of combinational logic can be reduced to a number of truth tables. As such, the upper bound on area was set at 274,080 LUTs.

## Interface Specifications

As shown in Figure 3.2, the computationally intensive part of the process of edge collision detection is finding points of intersection between an edge and the grids of the map. Comparing this result to an OGM is simple and fast. Therefore, it was decided that the hardware unit would simply take an edge and determine the grids with which it intersects. Whether the edge intersects a given grid can be represented as a binary  $\{0, 1\}$ , and thus a the intersections found in a  $\epsilon \times \epsilon \times \epsilon$  gridspace can be represented as an  $\epsilon^3$  sequence of binary values. Table 3.2 outlines the required interface specifications for the functional unit.

Element	Description/Justification
Constraints	
Length $\epsilon$	$\epsilon$ defines the max edge length. The space being checked and the output sequence has the dimensions $\epsilon \times \epsilon \times \epsilon$
Inputs	
Edge $e$	An Edge $e$ defined for a 3D configuration space by two points $\{p1, p2\}$ , each defined by a set of 3D coordinates $\{x, y, z\}$ .
Control Inputs	The functional unit must have ports for control signals: clock, reset, start. These are required for adding the unit to a processor.
Outputs	
Return Value	$\epsilon^3$ bit sequence: 1 if collides with grid at that index, 0 otherwise.
Control Outputs	Output ports for control signals: idle, done, ready. These are required for adding the unit to a processor.

Table 3.2: Interface Specifications for Edge Collision Detection Unit

### 3.2 HoneyBee



Figure 3.3: **Megalong Park Honey Bee Pollinating a Weeping Cherry Blossom.** Photographed by Emma Kenny in the Southern Highlands of New South Wales, Australia

The honey bee, *Apis mellifera*, has long been renowned for its tireless work ethic. However, the honey bee is rarely given credit for its remarkable navigation and collision avoidance strategies during flight. Recent research[13] suggests that honey bees, interestingly enough, explore their workspace randomly in order to find paths from their hive to sources of pollen. Sound familiar? As such, it is quite appropriate that this functional unit, designed to work tirelessly, rapidly and efficiently to execute collision detection computations for robot motion planning, was named **HoneyBee**.

HoneyBee is a hardware unit that will eventually be incorporated into a processor, demonstrated in Figure 3.4. In Chapter 4, the HoneyBee unit is implemented in a simple RISC-V processor and invoked using custom RISC-V instructions. For now, however, consider HoneyBee as a standalone unit that computes the grids with which an edge collides. Its resulting output can be compared to an OGM, as explained in section 3.1.1.

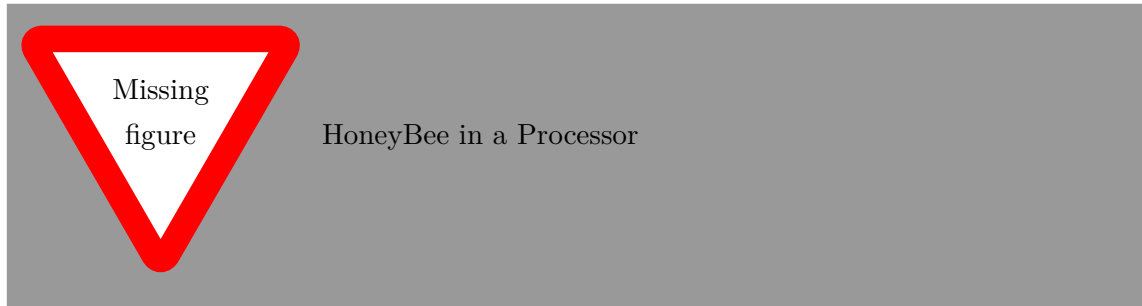


Figure 3.4

### 3.2.1 HoneyBee Interface Design

The interface for the HoneyBee functional unit, following on from the interface specifications outlined in Section 3.1.2 can be simply represented by Figure 3.5.

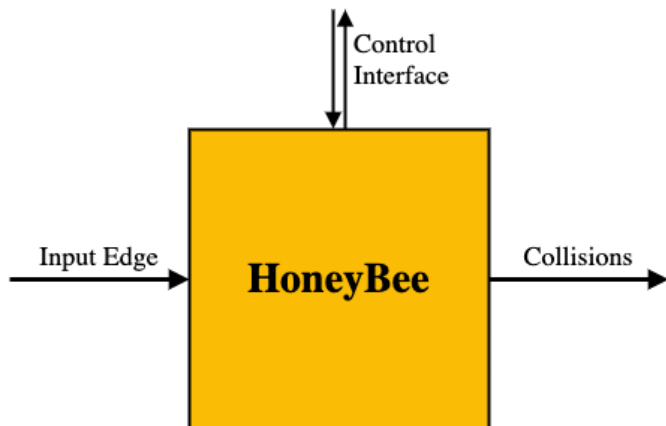


Figure 3.5: **General Overview of HoneyBee Interface.** The functional unit takes an edge  $e$ , defined by two points  $p_1$  and  $p_2$ , as an input, and outputs a series of collisions. These collisions describe which grids an edge intersects. Its control interface allows for communication with a processor's main control unit.

However, when designing hardware (the method of doing so is described in section 3.2.2), how these inputs and outputs are implemented must be considered at the bit level. Figure 3.6 shows all input, output, and control ports, and their bit-widths.

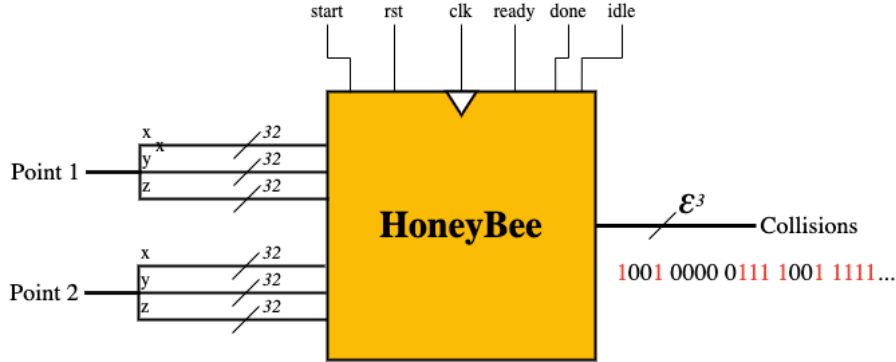


Figure 3.6: Port Diagram of HoneyBee Interface. The edge input is represented by 6 32-bit floats, following the IEEE 754 Single Precision 32-bit protocol, each float representing one of its coordinate points. The output sequence of collisions is a  $\epsilon^3$ -bit sequence, with each bit in the sequence representing one of the grids that was checked for intersections. It has input control signals for start and reset, and output control signals for done, idle, and ready. These control signals make up the necessary signals for a handshake protocol between HoneyBee and a processor's main controller.

## Inputs

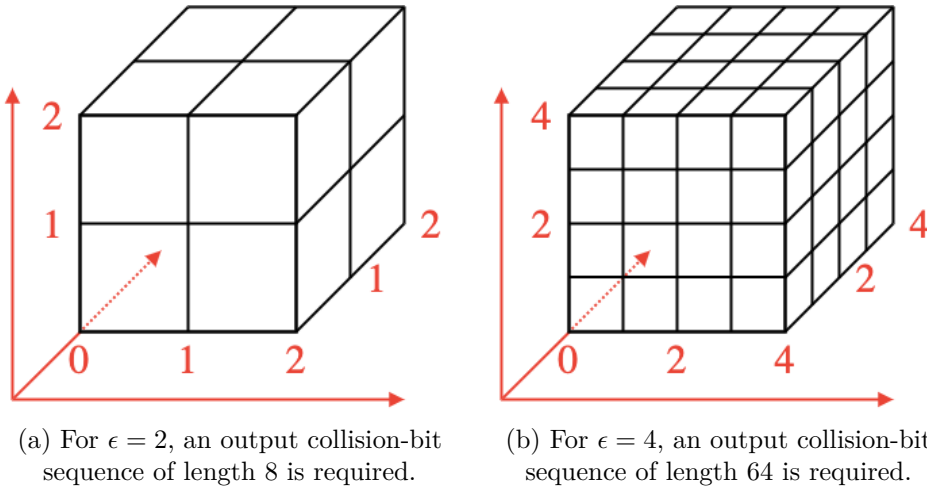
The inputs to HoneyBee collectively describe a single edge. This is done with 6 32-bit floating point numbers. How floating points (non-integer numbers) are represented in binary determined by the IEEE Standard for Floating-Point Arithmetic (IEEE754). How this is actually represented is not necessary to understand, but is explained in Appendix D.2. The important point is that the input edge determined by 6 32-bit coordinate points.

## Output

HoneyBee outputs a sequence of “collision-bits,” with each bit in the sequence representing if the input edge collides with its corresponding bit. How this sequence of bits is mapped to a 3D grid-map is explained in Appendix D.3. It is important to note that in the design and implementation of HoneyBee, the length of this sequence was parameterized to be variable, corresponding to a variable value of  $\epsilon$ . Recall that the optimal edge collision algorithm only checked  $\epsilon^3$  grids. HoneyBee, as well, only checks the grids with which the edge could possibly intersect.

Since the number of grids being checked is parameterized, so must the number of collision-bits be. This is demonstrated in Figure ??.

**Note:** The output bit-width is *parameterized* not *variable*. Upon synthesis (building) of HoneyBee, the output bit-width is set at a constant value. Different syntheses may have different output bit-widths. When the time comes to add HoneyBee to a processor, it is

Figure 3.7: The Impact of  $\epsilon$  on the Length of the Bit-Collision Sequence

synthesized with a certain bit-width.

### Control Interface

The control interface is designed to give HoneyBee the ability to be included in a processor, and implements a commonly used “handshake” protocol between HoneyBee and the control unit of the processor in which it resides. Put simply, this is a method that allows the control unit to tell HoneyBee when to start executing the computation, and for HoneyBee to tell the control unit when it has finished its computation and the output value is ready. This is explained in detail in Appendix D.4. The control interface also has a clock and reset port.

### 3.2.2 HoneyBee Implementation

#### Hardware Description Languages

Designing computers and their constituent parts has come a long way from its arduous beginnings. “Victory”, the enigma-breaking machine designed by Alan Turing at Bletchley Park during World War II, was a large electro-mechanical computer made up of storage wheels, electromagnetic relays, and rotary switches, assembled by hand.[14] So too was “Mark I”, the 816 cubic feet computer designed by Harvard University’s Dr. Howard Aiken, which, on March 1944, computed the viability of implosion for detonating the atomic bomb.[15]

Computers nowadays measure in the order of millimeters rather than meters. What’s more, they are now “built” in software, using a Hardware Description Language (HDL). HDLs is a family of computer programming languages that are used to specify the func-

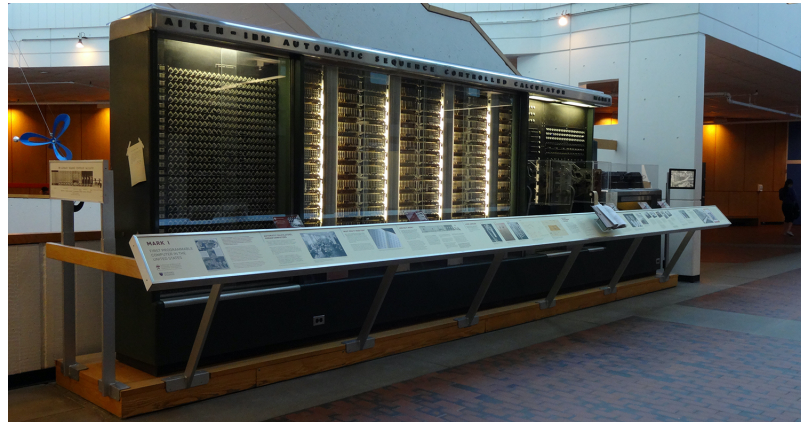


Figure 3.8: **The Harvard Mark I Computer**, photographed in the Harvard Science Center in April 2014 (Source: Harvard University)

tion of electronic circuits. Tools allow for simulation of such circuits to verify design correctness and performance. Modules defined in HDLs may then be synthesized for a type of integrated circuit called a Field Programmable Gate Array (FPGA). This FPGA, “programmed” in HDL code to behave in a certain way, can then serve the purpose of a processor or other functional processing unit. Figure ?? demonstrates this process.

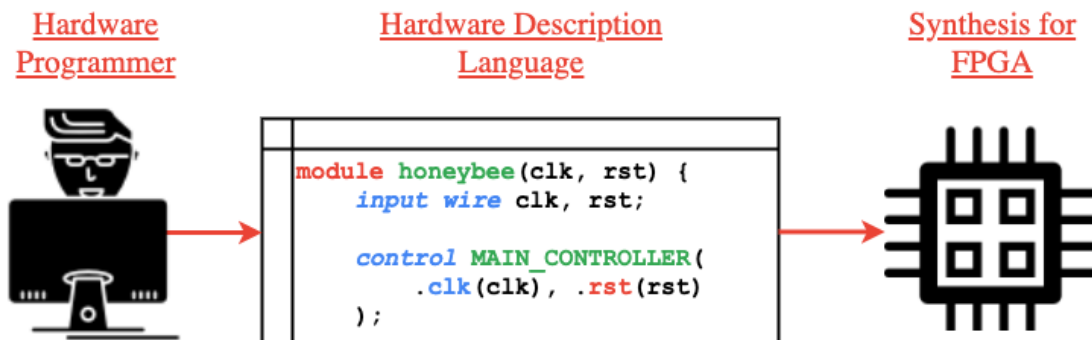


Figure 3.9: **The Hardware Development Process**, Defining Hardware Units in Hardware Description Languages for FPGAs.

HoneyBee was implemented eventually in an HDL called Verilog. However, no Verilog for HoneyBee was ever explicitly written by a human. It was generated by a tool called High-Level Synthesis.

## High Level Synthesis

High Level Synthesis (HLS) is an automated hardware design process that takes design files (written in high-level languages, such as C, C++ or SystemC) specifying the algorithmic function of a piece of hardware, interprets those files, and creates digital hardware designs that execute this function. In short, it effectively translates programming languages into hardware description languages. Some key advantages of using HLS are speed and verification. It is much faster and easier to define functionality in C than it is in a HDL such as Verilog, and thus design iterations are faster. It is also much simpler to verify one's design, as the functional units can be put through test benches written in C.

The most important benefit of using HLS, however, is the ability to use “pragmas.” These are simply directives given to the HLS tool that tell it what optimizations to use when translating C code into an HDL. This allows the same functionality to be synthesized in many different ways, optimizing the synthesis for speed, area, memory, etc. As such, the hardware development process now allows developers to experiment quickly with different ways to implement the same functionality. This is demonstrated graphically by Figure 3.10 on Page 38.

## HoneyBee-A Synthesis

With the functionality of HoneyBee implemented in C, the first optimization iteration (designated HoneyBee-A (HB-A)) was synthesized. HB-A had no pragmas, and was merely a basic hardware implementation of the defined functionality. HB-A and all subsequent iterations) synthesized correctly to the interface specifications (See Appendix D.5 for technical interface report of synthesis). Table 3.3 shows the result of HB-A’s synthesis compared with its performance and area specifications. Obviously, the synthesis is well below the area limit, but nowhere near the specified performance metrics. This is where the beauty of High-Level Synthesis optimization came in.

Metric	Specification	Synthesis Result
Latency ( $\mu$ seconds/edge)	0.9	6.66
Throughput (edges/second)	1,111,111	150,150
FPGA Area LUTs	274,080	10,593

Table 3.3: Synthesis Results for HB-A with  $\epsilon = 4$

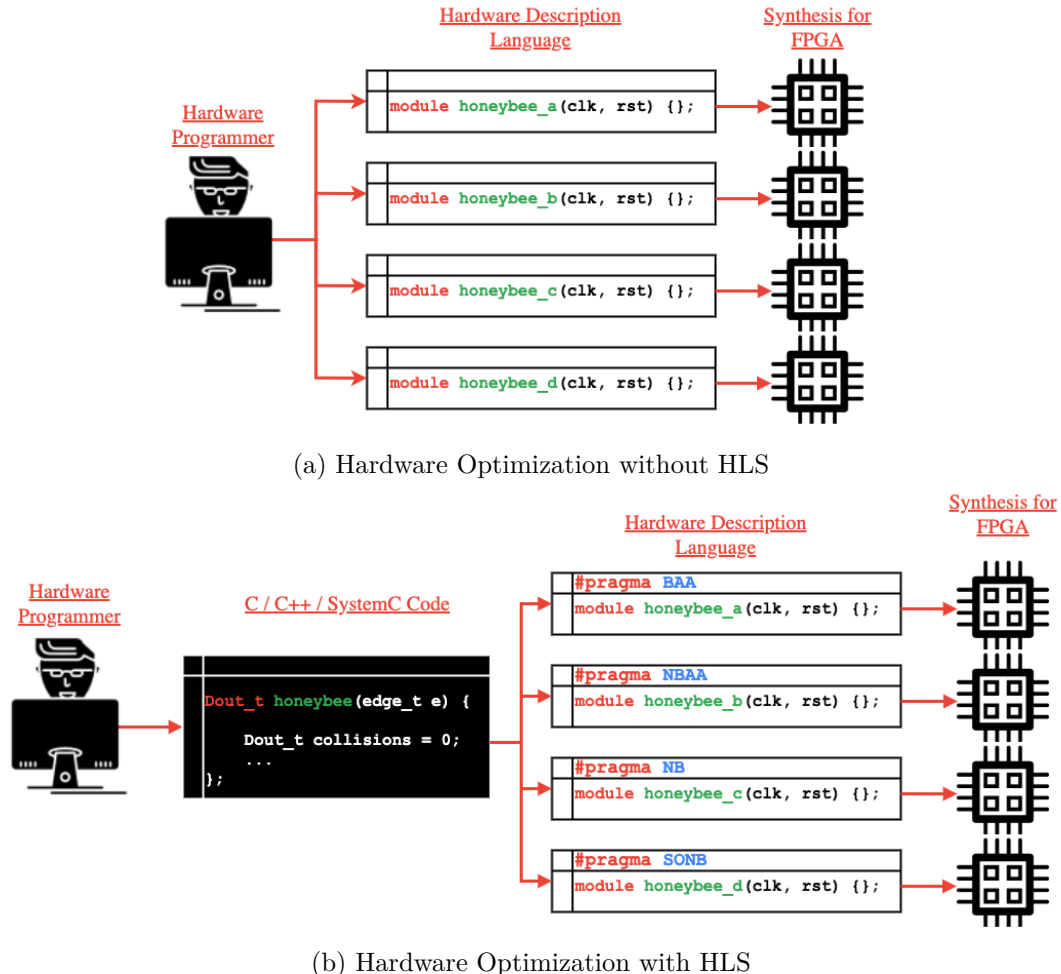


**Figure 3.10: Hardware Optimization Process.** Figure 3.10a shows how, without using HLS, the hardware developer must write multiple different implementation of the same functionality to achieve different performance. Figure 3.10b shows how, when using HLS, the hardware developer only must write one implementation (in a higher-level language like C), and then use “pragmas” to create different implementations (with different optimizations) for synthesis.

### 3.2.3 HoneyBee Acceleration

This section steps through the process of using HLS pragmas in 2 major optimization iterations, HoneyBee-B (HB-B) and HoneyBee-C (HB-C) and how these iterations compared to benchmark and specified performance.

#### Benchmarking

The benchmark performance was based on a Dual-Core Intel 3.1GHz i7 processor. In an ideal world, this processor would have been chosen after a rigorous process of determining the most suitable benchmark. In reality, this processor was chosen because it was the one found in the computer running the simulations (an early 2015 MacBook Pro). Nevertheless, it serves as a suitable benchmark, demonstrating performance typical of general purpose CPUs.

Examining latency, the benchmark was set at the average execution time for the benchmark CPU to compute 1 edge. Tests were run and averaged over 1000 trials. The average latency was  $2.6 \mu\text{seconds}$ , with a standard deviation of  $0.1 \mu\text{seconds}$ . This is shown, along with the performance of HB-A in Figure 3.11.

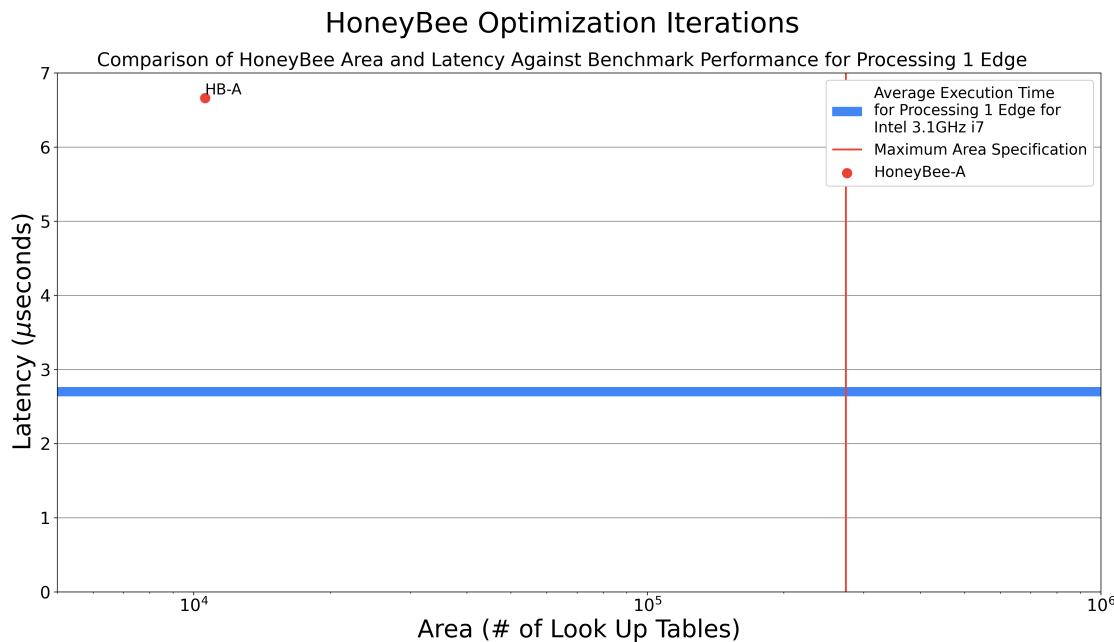
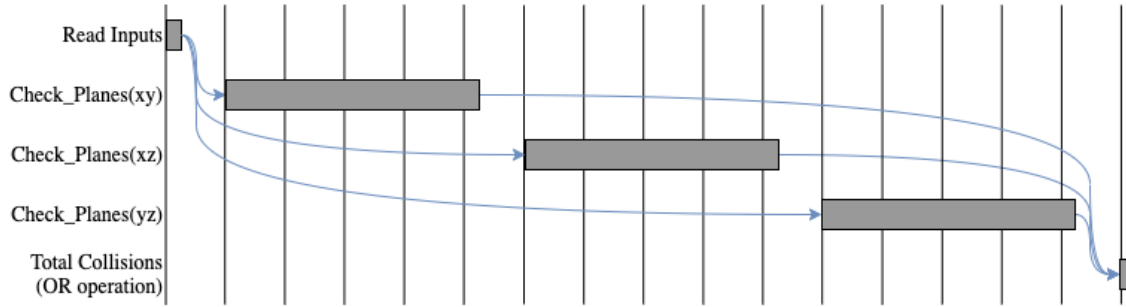


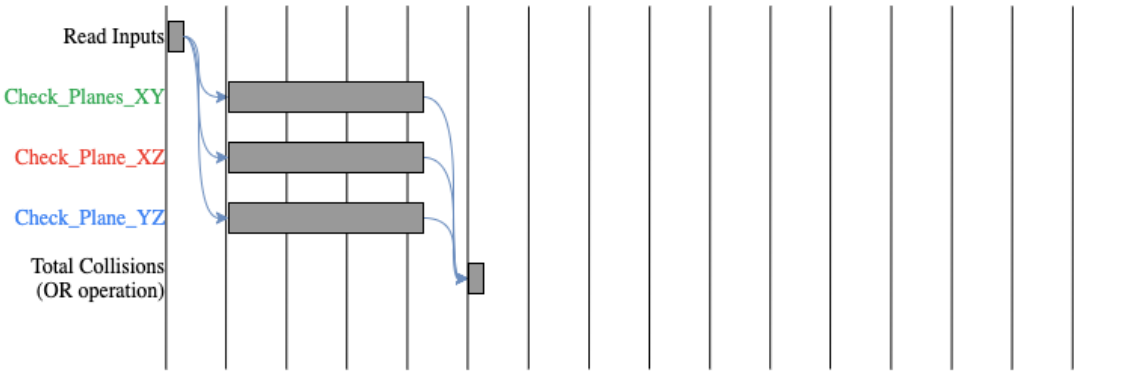
Figure 3.11: **HB-A Performance Against Benchmark CPU.** Standard deviation of CPU average performance is shown by width of the line for easier interpretation.

## HoneyBee-B

The first step in accelerating HoneyBee was taking advantage of the inherent parallelism available to the algorithm. Recall that the edge collision algorithm checks the  $xy$ -oriented planes, the  $xz$ -oriented planes, and finally the  $yz$ -oriented planes. These operations are completely independent, and can thus be performed simultaneously. Figure 3.14 shows how the process of checking each set of planes was done sequentially in HB-A, but are executed in parallel in HB-B.



(a) HoneyBee-A Timing Diagram. `Check_Planes` executed sequentially.



(b) HoneyBee-B Timing Diagram. `Check_Planes` executed in parallel. Different colors are to represent slightly different implementations of the same function.

Figure 3.12: **Timing Diagrams Showing Parallelization in HoneyBee-B**. Note these are generalizations for easy explanation of the concept of hardware parallelization. Full timing reports for each HoneyBee iteration can be found in Appendix D.6

The timing diagram does not only show the use of parallelism. It also shows how this is actually implemented in hardware. In HB-A (Figure 3.14a), there is a single module named `Check_Plane`. Since there is only one of them, it must calculate intersections with each set of planes sequentially. On the other hand, in HB-B (Figure 3.14b), there are three separate instances of this module (`Check_Planes_XY`, `Check_Planes_XZ`, and `Check_Planes_YZ`),

allowing HoneyBee to execute computation on all three sets of planes in parallel.

Moreover, notice that in HB-B, execution time of each of these three instances is shorter than that of the single instance in HB-A. When a single module instance is used for different purposes (in this case, checking the  $xy$ ,  $xz$ , and  $yz$  oriented planes), it has some variability. To control this variability, it must execute a certain amount of control logic at the beginning of the function. On the other hand, when there are separate instances of the module, what was once variable can now be made constant. As a result, each instance can be slightly specialized and the control logic eliminated. In this case, a general `Check_Planes` module was replaced with the three specialized `Check_Planes_XY`, `Check_Planes_XZ`, and `Check_Planes_YZ`. Each of these has less variability, thus less control logic, and therefore a slightly faster overall latency. Figure 3.14 shows how theoretically, this should result in a reduction in overall latency of more than 3 times.

Comparing HoneyBee-B against our benchmark, the success of this optimization can be seen. Figure 3.13 shows the performance of multiple variants of HB-B in yellow. These variants were the result of experimenting with slightly different pragmas, but all fell in roughly the same area. Appendix D.7 lists the details of each HB-B variant. HB-B3 showed the best performance/area relationship. It was of acceptable area and had latency marginally lower than the benchmark, but was not as fast as the defined specifications. Table 3.4 shows the result of HB-B3's synthesis compared with its performance and area specifications.

Metric	Specification	Synthesis Result
Latency ( $\mu$ seconds/edge)	0.9	2.05
Throughput (edges/second)	1,111,111	487,805
FPGA Area LUTs	274,080	26,524

Table 3.4: **Synthesis Results for HB-B3 with  $\epsilon = 4$**

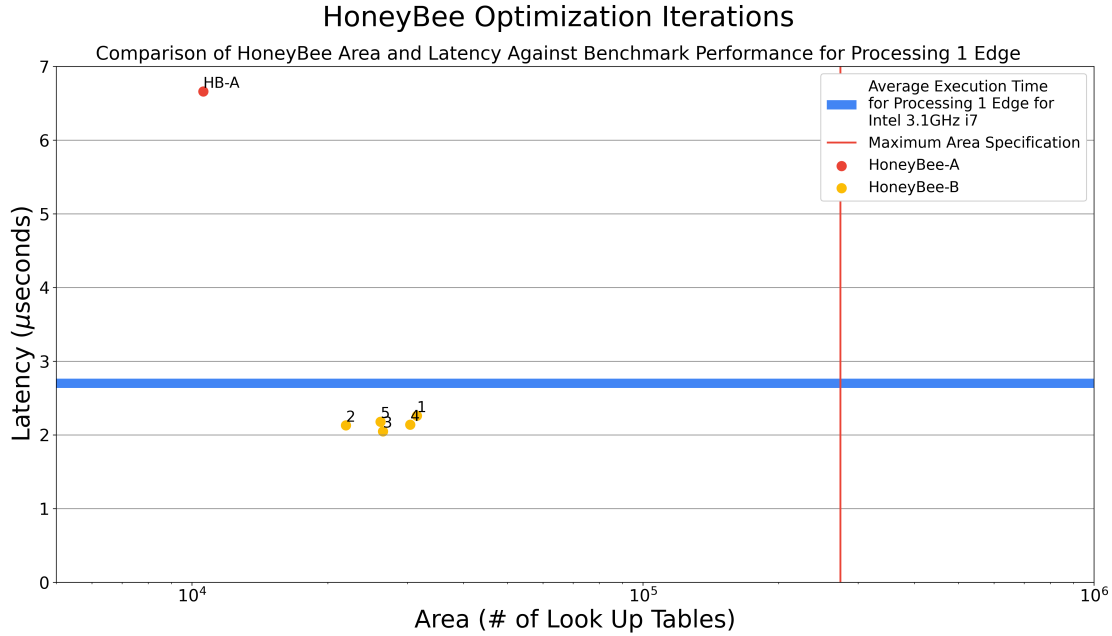
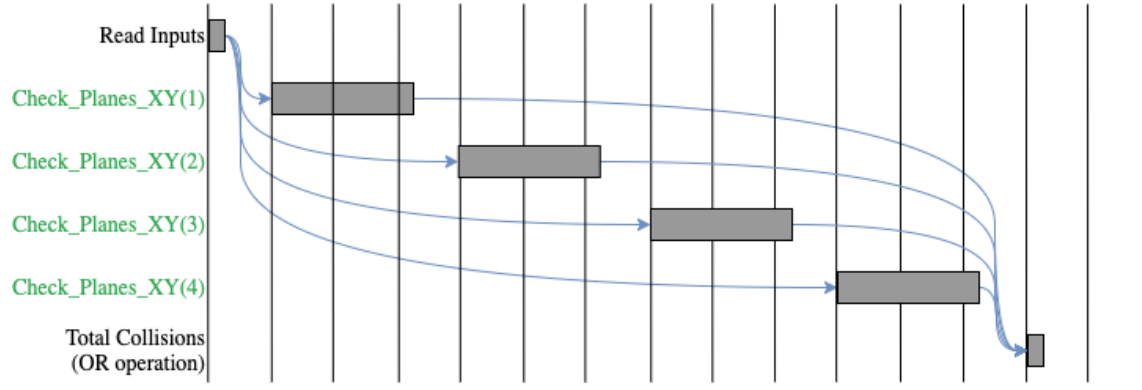


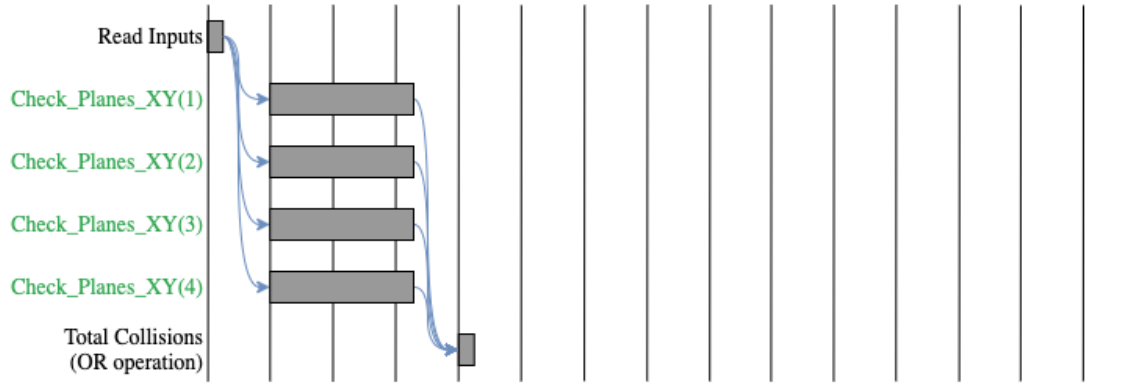
Figure 3.13: **HB-B Performance Against Benchmark CPU**  
Variants of HB-B shown in Yellow.

### HoneyBee-C

A similar concept was applied to optimize the computation of each set of planes. Consider synthesis of HoneyBee for  $\epsilon = 4$ . HoneyBee will need to compute intersections with 4  $xy$ -oriented planes, 4  $xz$ -oriented planes, and 4  $yz$ -oriented planes. HB-B computes each set of 4 planes simultaneously, but the computing intersections with each of the 4 planes in one orientation are also independent operations. As such, they can also be parallelized with the instantiation of more hardware modules. Figure ?? shows the timing diagrams for the `Check_Planes_XY` module that was shown in the last set of timing diagrams.



(a) HoneyBee-B Timing Diagram for `Check_Planes_XY`. One instance of `Check_Planes_XY` module executed sequentially 4 times ( $\epsilon = 4$ ).



(b) HoneyBee-C Timing Diagram. 4 instances of `Check_Planes_XY` module executing in parallel.

Figure 3.14: **Timing Diagrams Showing Parallelization in HoneyBee-C.** Again, these are generalizations for easy explanation of the concept of hardware parallelization.

Full timing reports for each HoneyBee iteration can be found in Appendix D.6

Just focussing on the computation of the *xy*-oriented planes, Figure ?? shows how HB-B than having one instance of the module execute 4 times sequentially. HB-C implements greater parallelism by instantiating 4 module instances to execute sequentially. HB-C, as a result, exceeded the performance benchmark and was of an acceptable area, as shown in Table 3.5 and Figure 3.15

Metric	Specification	Synthesis Result
Latency ( $\mu$ seconds/edge)	0.9	0.53
Throughput (edges/second)	1,111,111	1,886,792
FPGA Area LUTs	274,080	185,663

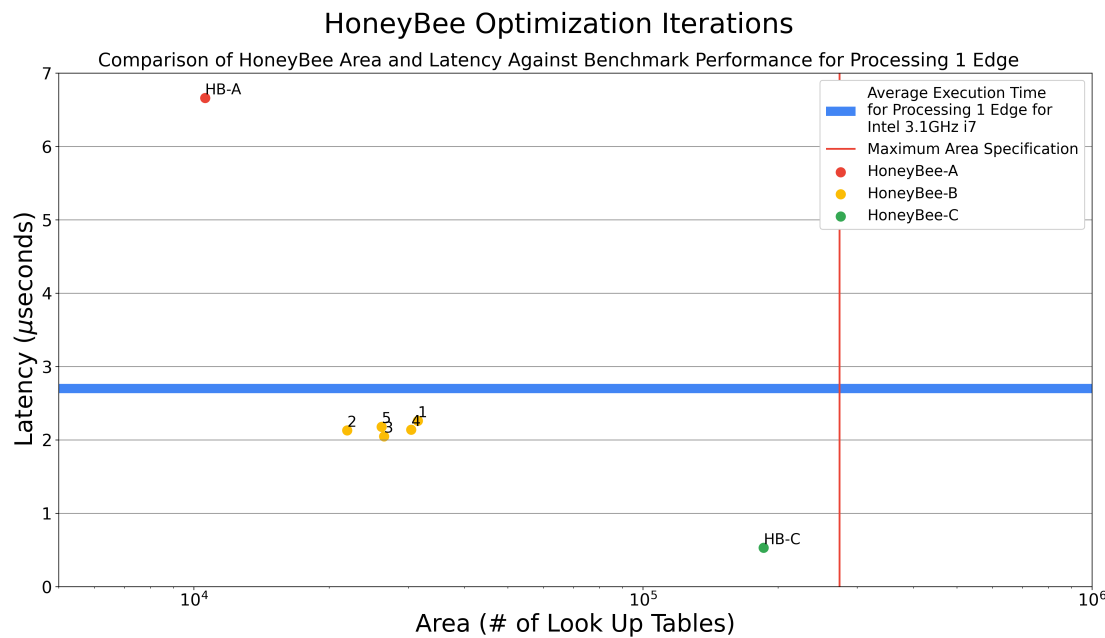
Table 3.5: Synthesis Results for HB-C with  $\epsilon = 4$ 

Figure 3.15:

## Chapter 4

# RISC-V Processor

Talk about determining honeybee output

Table 3.2 specifies that the edge collision unit takes an edge  $e$  with a maximum length of  $\epsilon$ . When implementing HoneyBee, it was necessary to determine a fixed value for  $\epsilon$ .

### 4.1 Introduction to the Reduced Instruction Set Computer

#### 4.1.1 Instruction Set Architecture

An Instruction Set Architecture can be thought of as an abstract model of a computer. On a broad level, it defines the data types, memory model, and registers of a computer, along with the instructions that it can execute.

It can also be thought as a “contract” between hardware and software developers. It is the promise made that the hardware will be able to execute all instructions defined in the ISA, and the limitation that software must be compiled into that set of instructions.

#### 4.1.2 RISC Processor Design

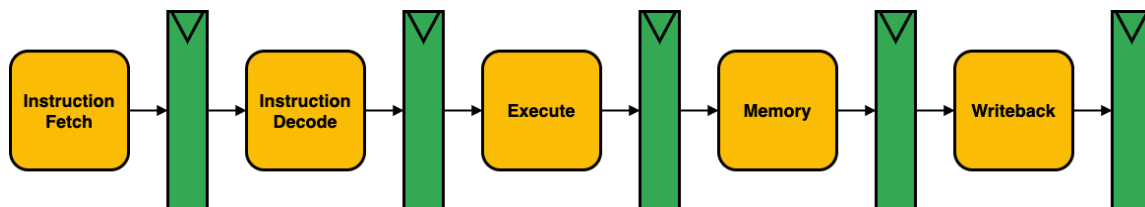


Figure 4.1: 5-Stage RISC Datapath

## 4.2 RISC-V ISA

### 4.2.1 RV32I

The following is an excerpt from the RISC-V Specification, outlining the RV32I base integer instruction set [7]

RV32I was designed to be sufficient to form a compiler target and to support modern operating system environments. The ISA was also designed to reduce the hardware required in a minimal implementation. RV32I contains 40 unique instructions, though a simple implementation might ...[reduce] base instruction count to 38 total. RV32I can emulate almost any other ISA extension ...

Subsets of the base integer ISA might be useful for pedagogical purposes, but the base has been defined such that there should be little incentive to subset a real hardware implementation ...

### Registers

RV32I defines 32 unprivileged registers, each 32 bits wide. They are designated  $x_0$ - $x_{31}$ , where  $x_0$  is a hard-wired value of 0, and registers  $x_1$ - $x_{31}$  hold values that various instructions use. RISC-V uses the load-store method, meaning that all operations perform on two registers or a register and an immediate, rather than performing operations directly on memory addresses. In addition, the 33rd unprivileged register is the program counter  $pc$ . Table 4.1 shows the register state for the RV32I Base Integer Instruction Set.

Register	ABI Name	Description
$x_0$	zero	Hard-wired zero
$x_1$	ra	Return address
$x_2$	sp	Stack pointer
$x_3$	gp	Global pointer
$x_4$	tp	Thread pointer
$x_5$ - $x_7$	t0-2	Temporaries
$x_8$	s0/fp	Saved register/Frame pointer
$x_9$	s1	Saved register
$x_{10}$ - $x_{11}$	a0-1	Function arguments/return values
$x_{12}$ - $x_{17}$	a2-7	Function arguments
$x_{18}$ - $x_{27}$	s2-11	Saved registers
$x_{28}$ - $x_{31}$	t3-6	Temporaries
$pc$	pc	Program counter

Table 4.1: Register State for RV32I Base Instruction Set

## Instruction Formats

Table 4.2 demonstrates the format of each different instruction type.

31	30	25 24	21	20	19	15 14	12 11	8	7	6	0	
		funct7		rs2		rs1	funct3		rd		opcode	R-type
		imm[11:0]			rs1	funct3		rd		opcode		I-type
		imm[11:5]		rs2		rs1	funct3	imm[4:0]		opcode		S-type
		imm[12]	imm[10:5]		rs2	rs1	funct3	imm[4:1]	imm[11]	opcode		B-type
		imm[31:12]						rd		opcode		U-type
		imm[20]	imm[10:1]	imm[11]	imm[19:12]			rd		opcode		J-type

Table 4.2: RV32I Base Instruction Formats

### 4.2.2 Motion Planning Extension

Motion Planning Extension: Full description of design of Non standard extension for motion planning. Should follow define, design, build, measure, analyse etc format.

## 4.3 PhilosophyV

*Philosophy IV*, written in 1903 by Mr. Owen Wister of the Class of 1882, recounts the antics of two Harvard students and their last minute attempts to study (or avoid studying) for an exam for which they are hopelessly unprepared. Similarly, this section details the process of my attempt to build a RISC-V processor, by far the most complex part of this Thesis, and a task for which I am unsure of my preparedness. As such, this processor is named Philosophy V; both in reference to the RISC-V ISA for which it is designed, and to the fact that my current situation seems much like a sequel to Mr. Wister's novel.

### 4.3.1 Baseline Implementation

Description of Baseline Philosophy V core

Figure 4.2 provides a schematic of the PhilosophyV processor.

Display bigger version of processor.

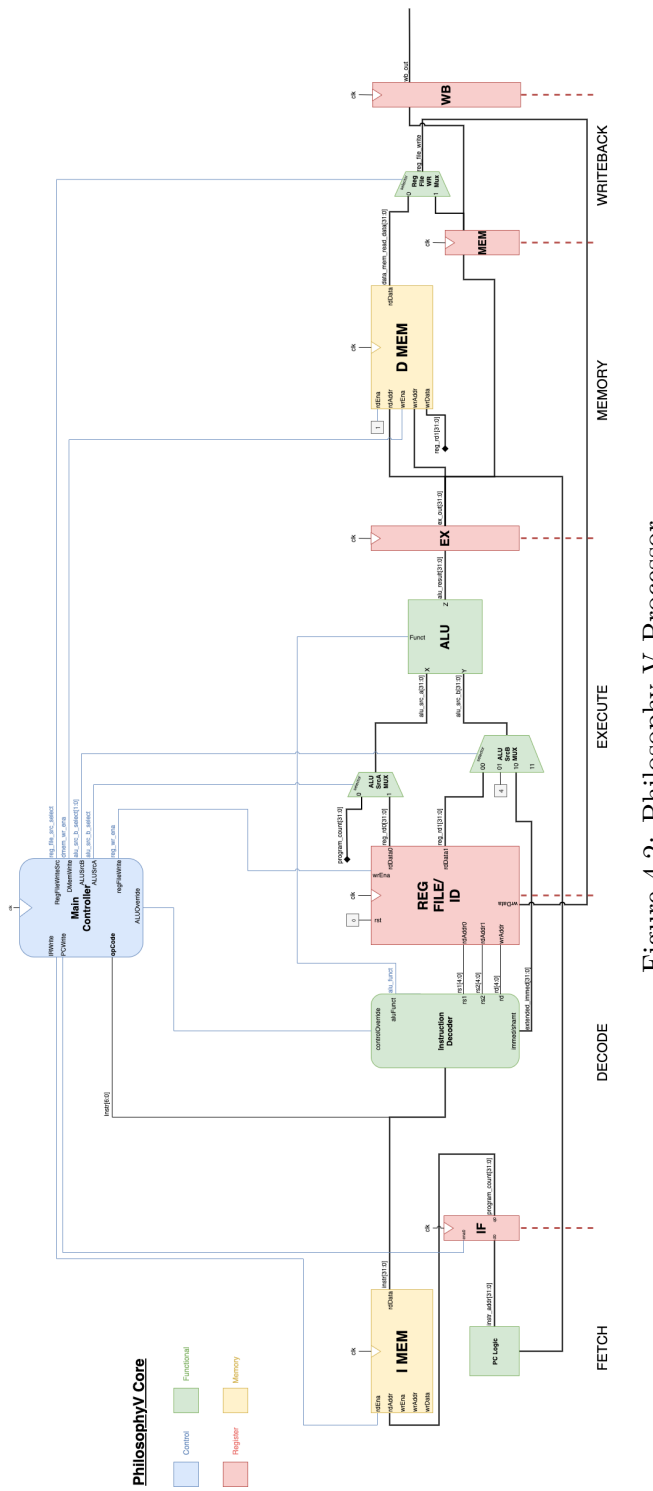


Figure 4.2: Philosophy V Processor

### 4.3.2 Implementing HoneyBee

Process of implementing honeybee into PhilV.

## 4.4 Performance Analysis

Comparative Performance Analysis of baseline and extended PhilV Core

# **Chapter 5**

## **Conclusion**

### **5.1 Discussion of Results**

Discussion of Results

### **5.2 Evaluation of Success**

Evaluation of Success

### **5.3 Future Work**

Future Work

# Bibliography

- [1] H. (Alexandrinus), *De gli automati, overo machine se moventi, Volume 2.*
- [2] V. I. B. U.-l. Isa, A. Waterman, Y. Lee, D. Patterson, K. Asanovi, and B. U.-l. Isa, “The RISC-V Instruction Set Manual v2.1,” *2012 IEEE International Conference on Industrial Technology, ICIT 2012, Proceedings*, vol. I, pp. 1–32, 2012.
- [3] N. Atay and B. Bayazit, “A motion planning processor on reconfigurable hardware,” in *Proceedings - IEEE International Conference on Robotics and Automation*, vol. 2006, pp. 125–132, 2006.
- [4] S. Murray, W. Floyd-Jones, G. Konidaris, and D. J. Sorin, “A Programmable Architecture for Robot Motion Planning Acceleration,” tech. rep.
- [5] G. S. Malik, K. Gupta, K. M. Krishna, and S. R. Chowdhury, “FPGA based combinatorial architecture for parallelizing RRT,” in *2015 European Conference on Mobile Robots, ECMR 2015 - Proceedings*, Institute of Electrical and Electronics Engineers Inc., nov 2015.
- [6] S. Murray, W. Floyd-Jones, Y. Qi, D. Sorin, G. Konidaris, and D. Robotics, “Robot Motion Planning on a Chip,” tech. rep.
- [7] A. Waterman, K. Asanovic, and SiFive Inc, “The RISC-V Instruction Set Manual,” vol. Volume I:, 2019.
- [8] C. E. Shannon, “XXII. Programming a computer for playing chess,” *The London, Edinburgh, and Dublin Philosophical Magazine and Journal of Science*, vol. 41, pp. 256–275, mar 1950.
- [9] M. Campbell, A. J. Hoane, and F. H. Hsu, “Deep Blue,” *Artificial Intelligence*, vol. 134, pp. 57–83, jan 2002.
- [10] S. M. LaValle, “Rapidly-Exploring Random Trees: A New Tool for Path Planning,” *In*, vol. 129, pp. 98–11, 1998.

- [11] S. M. LaValle and J. J. Kuffner, “Randomized kinodynamic planning,” *International Journal of Robotics Research*, vol. 20, pp. 378–400, may 2001.
- [12] Intel, “VTune Profiler,” 2019.
- [13] R. Menzel, U. Greggers, A. Smith, S. Berger, R. Brandt, S. Brunke, G. Bundrock, S. Hülse, T. Plümpe, F. Schaupp, E. Schüttler, S. Stach, J. Stindt, N. Stollhoff, and S. Watzl, “Honey bees navigate according to a map-like spatial memory,” *Proceedings of the National Academy of Sciences of the United States of America*, vol. 102, pp. 3040–3045, feb 2005.
- [14] “The man who knew too much: Alan Turing and the invention of the computer,” *Choice Reviews Online*, 2006.
- [15] F. Elsabbagh, B. Asgari, H. Kim, and S. Yalamanchili, “Vortex RISC-V GPGPU System: Extending the ISA, Synthesizing the Microarchitecture, and Modeling the Sooware Stack,” tech. rep., 2019.
- [16] Thingbits, “LynxMotionHQuad500 Drone.”
- [17] RoboJackets, “RRT,” 2019.  
<https://github.com/RoboJackets/rrt>.
- [18] M. Planning, “rrt-algorithms,” 2019.  
<https://github.com/motion-planning/rrt-algorithms>.
- [19] Sourishg, “rrt-simulator,” 2017.  
<https://github.com/sourishg/rrt-simulator>.
- [20] Vss2sn, “Path Planning,” 2019.  
[https://github.com/vss2sn/path\\_planning](https://github.com/vss2sn/path_planning).
- [21] Olzhas, “RRT Toolbox,” 2017.
- [22] Xilinx, “Vivado Design Suite User Guide for High-Level Synthesis,” tech. rep., 2014.

# Glossary

**RISC-V:** (Pronounced “risk-five”) is an open-source and extendible ISA developed by the University of California, Berkeley. It is established on the principles of a RISC, a class of instruction sets that allow a processor to have fewer CPI than a CISC.

**A priori:** relating to or denoting reasoning or knowledge which proceeds from theoretical deduction rather than from observation or experience..

**Automata:** moving mechanical devices made in imitation of human beings.

**Axis-oriented plane:** Planes that run parallel to one of the  $xy$  plane, the  $xz$  plane, or the  $yz$  plane..

**Bit-width:** The number of binary digits necessary to represent a data type. For instance, a boolean takes 1 bit (1 or 0), whereas an integer may be represented by any number of bits (most commonly 32).

**Bit:** A binary digit, 1 or 0, and the most basic unit of information in computing. Bits are combined to represent complex information. Every single thing your computer does is, eventually, represented and implemented in the movement of bits..

**Configuration:** A specification of a robots location, position, and setting in a space. For example, when a robot is represented by a single point in 3D space, its configuration is merely x, y, and z coordinates. But if a robot is represented as a 3D humanoid with a head, body, arms and legs, then its configuration would be its position in 3D space, its orientation in 3D, and the position of all its joints and limbs such that the space being taken up by the robot can be exactly determined. It is obvious then that as the physical complexity of a robot increases, so too does the complexity of representing it algorithmically..

**Dijkstra’s algorithm:** An algorithm for finding the shortest path between two nodes in a graph..

**Hardware acceleration:** The process of speeding up the execution of a function by implementing part or whole of that function specifically in hardware..

**Mathematically complete:** An algorithm is mathematically complete if it will always find all solutions..

**Pragma:** From the word “pragmatic”. A programming directive that specifies how the relevant code should be processed. In the context of HLS, they are the directives that can be used to optimize how C Code is synthesized into HDL.

**Probabilistically complete:** Describes an algorithm with a likelihood of finding a solution that approaches one as its runtime approaches infinity..

**Real-time:** Describes a system in which input data is processed in such a time period such that it is available almost immediately. Systems such as missile guidance or collision avoidance in cars are an example of real-time systems.

**Time complexity:** Refers to the amount of time taken by an algorithm to run as a function of the length of its input.

**Workspace:** The space which a robot and obstacles occupy in motion planning problems.

**Advanced RISC Machine (ARM):** A family of Reduced Instruction Set Computing architectures for computer processors, configured for various environments..

**Application Specific Processor (ASP):** A computer processor that has been optimized for a specific function or set of functions that support a given application..

**Complex Instruction Set Computer (CISC):** A computer in which single instructions can execute several low-level operations (such as a load from memory, an arithmetic operation, and a memory store) or are capable of multi-step operations or addressing modes within single instructions..

**Degree-of-Freedom (DOF):** Refers to the number of independent factors that describe the configurations in which a robot can exist and motion can occur..

**Field Programmable Gate Array (FPGA):** An integrated circuit designed to be configured by a designer after manufacturing – hence the term ‘field-programmable’. Its behaviour is specified in software, using a HDL.

**Hardware Description Language (HDL):** A computer language used for designing computer hardware. It is used to define the behaviour of modules, simulate their performance, and synthesize them on an FPGA.

**High Level Synthesis (HLS):** An automated hardware design process that takes software written in high-level languages (often C, C++) that algorithmically defines a function, and converts that into HDL that implements that function..

**IEEE Standard for Floating-Point Arithmetic (IEEE754):** The technical standard for how floating-points are represented and processed in binary, established by the Institute of Electrical and Electronics Engineers..

**Instruction Set Architecture (ISA):** An abstract model of a computer, that defines the instructions, registers, memory behaviour, and other attributes of a computer architecture. It can be thought of as the contract between software and hardware developers, as the ISA lists the instructions that software may be implemented in, and the instructions that a processor must support..

**Look-Up Table (LUT):** This is a “truth-table” used in FPGAs that determine what output to return for a given input. Any amount of combinational logic can be reduced to a number of truth tables..

**Occupancy Grid Map (OGM):** A method of representing a 2D or 3D space by dividing it into discrete grids and marking each whole grid as occupied; even if only part of it is..

**Probabilistic Road Map (PRM):** A motion planning algorithm that randomly samples free space, and then connects sampled configurations with nearby configurations to build a map..

**Reduced Instruction Set Computer (RISC):** A computer architecture based on a small number of instructions executed in a small number of cycles..

**Rapidly-exploring Random Tree (RRT):** an algorithm designed to efficiently search, and thus plan a path through, a high-complexity environment by randomly sampling points and building a tree. The algorithm randomly samples points, draws an edge from the nearest currently existing node in the tree, to grow the tree in the space..

**Real-Time Operating Systems (RTOS):** A type of operating system designed to operate on inputs as they come in, without buffer delays..

**RISC-V 32-Bit Integer (RV32I):** One of the four base ISAs within RISC-V. While it implements integer values only in 32-bit representations, it contains the minimal number of instructions for a fully working computer processor..

**System on Chip (SoC):** A chip that includes all required components of a working computer, including one or more CPUs, memory, I/O ports, etc..

**Unmanned Aerial Vehicle (UAV):** An aircraft without a human pilot on board. It may be piloted remotely completely by a human pilot, autonomously pilot itself, or a mixture of the two..

# Appendices

# Appendix A

# Project Repository

This project's repository can be found at [github.com/AnthonyKenny98/Thesis](https://github.com/AnthonyKenny98/Thesis) and contains multiple subrepositories. It has the following structure.

## Research

This folder holds the academic papers that constitute the background research of this Thesis.

## Writeups

This folder holds the writeups required for this Thesis, including checkpoints in fulfillment of Harvard's ES100hf class and this Final Report

## RRT

[github.com/AnthonyKenny98/RRT](https://github.com/AnthonyKenny98/RRT)

This subrepository holds both the 2D and 3D implementations of RRT used for this thesis, along with the tools required for both VTune Profiler and internal timing analysis.

## HoneyBee

[github.com/AnthonyKenny98/HoneyBee](https://github.com/AnthonyKenny98/HoneyBee)

This subrepository holds the HoneyBee functional unit, a hardware implementation of collision detection.

## PhilosophyV

[github.com/AnthonyKenny98/PhilosophyV](https://github.com/AnthonyKenny98/PhilosophyV)

This subrepository holds the PhilosophyV RISC-V chip

## **Appendix B**

### **Budget**

Budget

## Appendix C

# RRT Supporting Documentation

### C.1 Justification of Modelling UAV as Prism

While it is possible for a UAV to be modelled in precise detail, taking into account its exact shape, more often UAVs are modelled as a 3D prism in motion planning problems, for the following reasons:

- It is a rare case that the negative space gained by modelling in such detail is utilised
- Representation of the drone's configuration is much more complex.
- Computing edge collisions is much more computationally intensive.

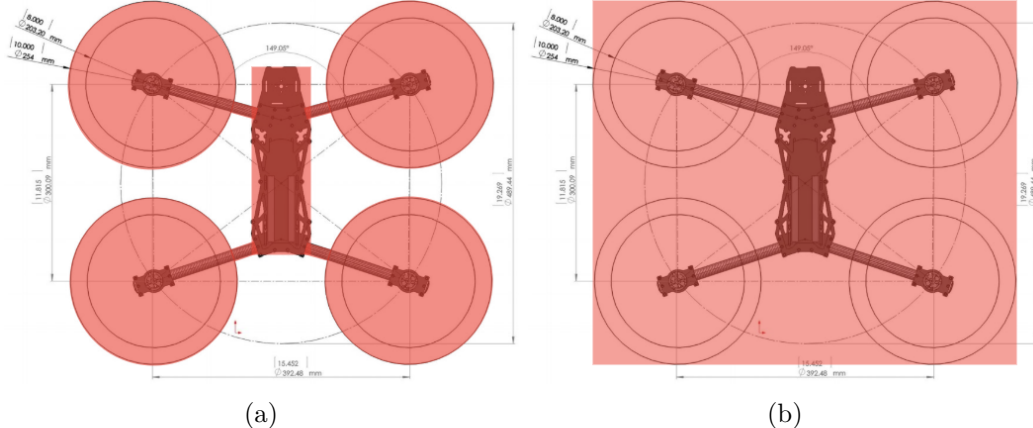


Figure C.1: **Modelling a UAV as a Rectangular Prism.** Red highlights demonstrate the configuration model, overlayed over the exact schematic. Figure C.1a shows how a drone can be modelled in high detail, but gains little useful free space when compared with Figure C.1b, which models a drone as a rectangular prism.[16]

## C.2 Full Technical Specifications for RRT Implementation

General Specifications	
Requirement	Description and Justification
Implemented in C/C++	As outlined in Section 1.3.3, the critical step in determining the design of specialized hardware to accelerate RRT is CPU performance analysis of the algorithm to determine computational hot-spots. Implementations in C allow for the use of certain CPU profiling tools, unlike higher-level languages such as Python.
3D Workspace	The computational requirements of RRT in 3D differs somewhat to that in 2D. Since autonomous UAVs operate in 3D space, it was necessary to have a 3D implementation to analyse.
UAV modelled in 3D as a rectangular prism	In theory, it is possible to model a UAV much more precisely than a rectangular prism, taking into account its shape and negative space. However, in reality, modelling a UAV as a 3D rectangular prism, defined by coordinates $\{x, y, z\}$ and Euler angles $\{\alpha, \beta, \gamma\}$ , is more than sufficient (and more efficient). See Appendix C.1 for justification of this.
Mathematically Complete Collision Detection	When RRT is implemented for educational purposes, the edge collision calculations are often simplified to a sampling model which is probabilistically complete but not mathematically complete. In other words, it will catch most collisions by sampling a number of points along each edge, but there is always a possibility of an undetected collision. In real world applications, collisions must be calculated by method of geometric intersection to ensure all collisions are detected.

Table C.1: General Technical Specifications for RRT Implementation

Required Parameters	
Parameter	Description and Justification
$\epsilon$ (a.k.a. $\Delta q$ )	The maximum difference between two configurations. Larger values of $\epsilon$ can solve less obstacle dense problems faster, but take longer to solve problems with tight corners.
$K$	The maximum number of configurations. This is largely correlative to the amount of time the user will allow the algorithm to run. Larger values of $K$ will take longer but generate better paths, while smaller values will execute for less time but generate more jagged paths or may not reach the goal node. The value of $K$ was varied to find the minimum execution time while still reaching the goal with high probability.
$DIM$	The upper bound of each axis of a $DIM \times DIM \times DIM$ Workspace. Larger values leave more space to be explored, and thus require larger values of $K$ to reach the goal with high likelihood.
Goal Bias	The given probability that the graph will extend the graph $\epsilon$ distance from an existing configuration to a new configuration in the direction of the goal.

Table C.2: Required Parameters for RRT Implementation

### C.3 Assessment of Existing RRT Implementations

	General Requirements					Parameters			
	Language	2D/3D	Object Model	Collision Detect	$\epsilon$	$K$	$DIM$	Goal Bias	
RoboJackets[17]	C++	2D	Point	Complete	Yes	Yes	Yes	No	
Motion-Planning[18]	Python	ND	Point	Incomplete	Yes	Yes	No	Yes	
Sourishg[19]	C++	2D	Point	Incomplete	Yes	Yes	No	No	
Vss2sn[20]	C++	2D	Point	Complete	Yes	Yes	No	No	
olzhas[21]	Matlab	2D	Point	Complete	Yes	Yes	No	No	

Table C.3: Evaluation of Existing Open-Source Implementations of RRT. Links to Github repositories can be found in the Bibliography.

## C.4 Implementation of Key RRT Functions

---

**Algorithm C.1:** `getRandomConfig()` as implemented for RRT

---

**Inputs:** Dimensionality  $N$ ,  
Upper Axis Bound  $DIM$

**Output:** Random Configuration  $q$

```

 $q.x \leftarrow \text{randomFloat}(DIM)$ 
 $q.y \leftarrow \text{randomFloat}(DIM)$ 
 $q.\alpha \leftarrow \text{randomFloat}(2\pi)$ 
if  $N == 3$  then
     $q.z \leftarrow \text{randomFloat}(DIM)$ 
     $q.\beta \leftarrow \text{randomFloat}(2\pi)$ 
     $q.\gamma \leftarrow \text{randomFloat}(2\pi)$ 
end
return  $q$ ;
```

---

Where `randomFloat(max)` returns a float between 0 and `max`.

---

**Algorithm C.2:** `findNearestConfig()` as implemented for RRT

---

**Inputs:** Graph  $G$ ,  
New Configuration  $q_{new}$

**Output:** Nearest Configuration  $q_{nearest}$

```

 $q_{nearest} \leftarrow G.q_{init}$ 
for  $k = 0$  to  $G.\text{existing\_nodes}$  do
    if  $\text{distance}(q_{new}, G.q[k]) < \text{distance}(q_{new}, q_{nearest})$  then
         $| q_{nearest} \leftarrow G.q[k]$ 
    end
end
return  $q_{nearest}$ 
```

---

Where `distance( $q_1$ ,  $q_2$ )` returns the Euclidean distance between two configurations.

---

**Algorithm C.3: stepFromNearest()** as implemented for RRT

---

**Inputs:** Configuration in Graph  $q_{nearest}$ ,  
 New Configuration  $q_{new}$ ,  
 Goal Bias  $B$ ,  
 Maximum Step Distance  $\epsilon$ ,  
 Graph  $G$

**Output:** Updated New Configuration  $q_{new}$

```

if distance( $q_{nearest}, q_{new}$ ) >  $\epsilon$  then
  if randomFloat(1) <  $B$  then
    |  $q_{new} \leftarrow \text{stepTowardConfig}(q_{nearest}, G.q_{goal})$ 
  end
  else
    |  $q_{new} \leftarrow \text{stepTowardConfig}(q_{nearest}, q_{new})$ 
  end
end
return  $q_{new}$ ;
```

---

Where  $\text{stepTowardConfig}(q_1, q_2)$  returns a configuration  $\epsilon$  from  $q_1$  in the direction of  $q_2$ .

---

**Algorithm C.4: configCollision()** as implemented for RRT

---

**Inputs:** Dimensionality  $N$ ,  
 Occupancy Grid Map ( $N$ -Dimensional Array)  $O$ ,  
 Configuration  $q$

**Output:** Boolean

```

if  $N == 2$  then
  | return  $O[\text{gridLookup}(q.x)][\text{gridLookup}(q.y)]$ 
end
else
  | return  $O[\text{gridLookup}(q.x)][\text{gridLookup}(q.y)][\text{gridLookup}(q.z)]$ 
end
```

---

Where  $O$  is a  $N$ -Dimensional array of booleans, with True representing an occupied grid and false representing an unoccupied one.  $\text{gridLookup}()$  is a function that maps a floating point coordinate to the correct integer of the grid in which it resides. For a map resolution of one, this is as simple as rounding a float down to an integer.

While seemingly complex, the above algorithm merely steps through the mathematical process of checking the relevant  $x$ ,  $y$ , and  $z$  planes for a point of intersection with the

---

**Algorithm C.5: configCollision()** as implemented for RRT for 3D

---

**Inputs:** Edge  $e$ ,  
     Occupancy Grid Map (3-Dimensional Array)  $O$ ,  
     Maximum Step Distance  $\epsilon$

**Output:** Boolean

```

 $q_{min} \leftarrow \text{minConfig}(e.q_1, e.q_2)$ 
for ( $x = q_{min}.x$  to  $q_{min}.x + \epsilon$ ) do
     $q_{intersection} \leftarrow \text{edgeIntersectsPlane}(e, x)$ 
    if  $O[q_{intersection}.x][q_{intersection}.y][q_{intersection}.z]$  then
        return true
    end
end
for ( $y = q_{min}.y$  to  $q_{min}.y + \epsilon$ ) do
     $q_{intersection} \leftarrow \text{edgeIntersectsPlane}(e, y)$ 
    if  $O[q_{intersection}.x][q_{intersection}.y][q_{intersection}.z]$  then
        return true
    end
end
for ( $z = q_{min}.z$  to  $q_{min}.z + \epsilon$ ) do
     $q_{intersection} \leftarrow \text{edgeIntersectsPlane}(e, z)$ 
    if  $O[q_{intersection}.x][q_{intersection}.y][q_{intersection}.z]$  then
        return true
    end
end
return false

```

---

edge  $e$ . It then looks up the OGM  $O$  to see if the grid corresponding with the point of intersection is occupied. If so, then it reports a collision by returning false. The function `edgeIntersectsPlane` follows the geometrical process of detecting a segment-plane intersection outlined in Appendix C.5.  $q_{min}$  is calculated to be the origin point of the grid closest to the origin. In other words, the algorithm does not check for intersections throughout the entire map, only the maximum number of grids that could possibly be intersected by the edge  $e$ , given the location of the two points of the edge,  $e.p_1$  and  $e.p_2$ , and the maximum edge length  $\epsilon$ . The algorithm for `edgeCollision` in 2D can be inferred from the above, instead checking segment-line intersections for  $x$  and  $y$  lines.

## C.5 Geometrically Determining Segment-Plane Intersection

The method of edge collision detection in this project's implementation of RRT relies on detecting segment-plane intersections. The planes are always set up to be parallel with either the  $xy$  plane, the  $xz$  plane, or the  $yz$  plane. Figure C.2 demonstrates this point.

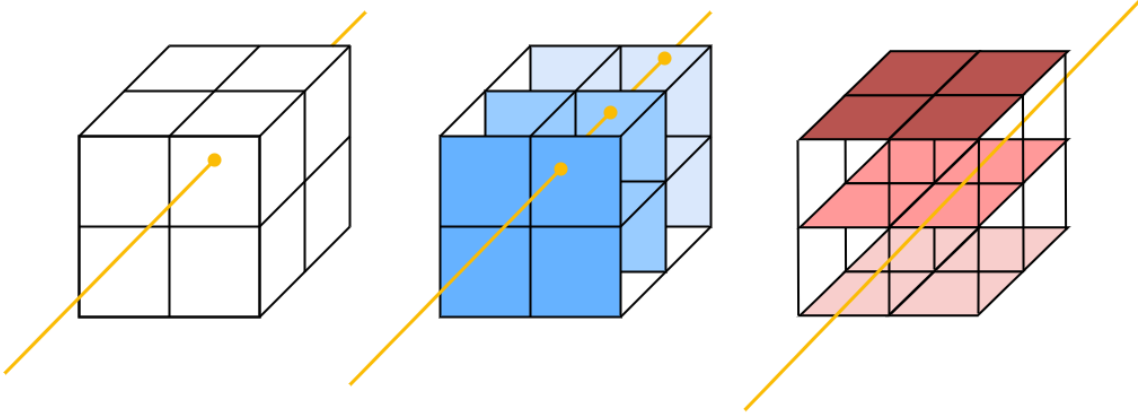


Figure C.2: Using Parallel Planes to determine Edge Collisions with Grids

A plane can be defined by 3 points,  $P_a$ ,  $P_b$ , and  $P_c$ . In practice, the points defining a plane parallel to the  $xy$  plane would have the following points:

$$P_a = (x, y, z)$$

$$P_b = (x + \Delta x, y, z)$$

$$P_c = (x, y + \Delta y, z)$$

Two vectors,  $\vec{AB}$  and  $\vec{AC}$  can be determined.

The normal to the plane is the cross product:

$$\vec{AB} \times \vec{AC}$$

And the equation of the plane written as:

$$a(x - x_0) + b(y - y_0) + c(z - z_0) = 0$$

$$ax + by + cz = ax_0 + by_0 + cz_0$$

Where  $\langle a, b, c \rangle$  is the normal to the plane and  $(x_0, y_0, z_0)$  is one of the points  $P_a$ ,  $P_b$ , or  $P_c$ . The RHS can be set to equal  $d$ , leaving:

$$ax + by + cz = d$$

Now, the equation of a line can be written in the form:

$$ax + by + cz = 0$$

And can be parameterized in the following form:

$$\begin{cases} x = x_1 + t(x_2 - x_1) \\ y = y_1 + t(y_2 - y_1) \\ z = z_1 + t(z_2 - z_1) \end{cases}$$

To find the point of intersection, we substitute the equation of the line into the equation of the plane, yielding:

$$a(x_1 + t(x_2 - x_1)) + b(x_1 + t(x_2 - x_1)) + c(x_1 + t(x_2 - x_1)) = d$$

Rearranging to find an expression for  $t$ :

$$t = \frac{d - (ax_1 + by_1 + cz_1)}{a(x_2 - x_1) + b(y_2 - y_1) + c(z_2 - z_1)}$$

Knowing  $t$ , we can find the point of intersection,  $P_X$  to be:

$$\begin{cases} x_X(t) = x_1 + t(x_2 - x_1) \\ y_X(t) = y_1 + t(y_2 - y_1) \\ z_X(t) = z_1 + t(z_2 - z_1) \end{cases}$$

Finally, the following equalities are evaluated to see if the point lies on the segment:

$$x_1 \leq x_X \leq x_2$$

$$y_1 \leq y_X \leq y_2$$

$$z_1 \leq z_X \leq z_2$$

If so, then the grids corresponding to the point of intersection can be marked as intersected.

## C.6 Timing Methodology of RRT Analysis

### VTune Profiler

VTune Profiler is an application for software performance analysis. It provides functionality to examine hot-spots for CPU execution time through a top down analysis. The top down analysis tool shows the percentage of CPU time taken up by each function. It was used to initially profile the algorithm's performance.

## Internal Timing

There are several limitations to using VTune Profiler. First, it can only profile software running on Intel processors, which implement the x86 ISA. In anticipation of potentially needing to run performance analysis on a RISC-V processor, another method was required. Secondly, VTune Profiler takes a long time to run, as it needs to conduct a lot of analysis that is extraneous to the purpose of this thesis. This became prohibitive when it came to conducting hundreds of tests for different parameterizations, with each test running RRT a minimum of 100 times. Finally, it was not customizable to ignore certain parts of the implementation, such as logging functionality. While the implementation was designed in such a way that these should not interfere, it led to a lot of irrelevant data. A simple and effective alternative for measuring execution performance was to insert timing functionality into the software itself.

Internal timing was implemented based on the inbuilt C `clock()` function and `CLOCKS_PER_CYCLE` macro, and wrapping each function of interest in a performance tracking struct. This can be seen in the project's RRT sub-repository under `performance.h`.

## Comparison

Before proceeding to use the internal timing method, it was important to verify that this method yielded similar results to VTune Profiler for the same program. Table C.4 summarizes the results of analysis of a simple C executable. The program calls 5 functions,  $\{A, B, C, D, E\}$ , each a simple iteration in which a integer is incremented. Since the Internal Timing method returned similar results to the (trusted) VTune Profiler, it was considered to be a reliable method. While it was encouraging to see both methods returned similar results for absolute execution time, the more important metric was the similarity in percentage of total execution time. For good measure, a  $\chi^2$  test of hypothesis was conducted and for one degree of freedom showed more than acceptable results.

function	Vtune Profiler		Internal Timing		$\chi^2$
	time (s)	time (% total)	time (s)	time (% total)	
A	0.488	57.4%	0.497	57.6%	0.00016
B	0.2	23.5%	0.198	23.1%	0.00002
C	0.102	12.0%	0.099	11.5%	0.00009
D	0.048	5.7%	0.049	5.6%	0.00002
E	0.012	1.4%	0.019	2.2%	0.00408

Table C.4: Comparison of Timing Methods

## **Appendix D**

# **HoneyBee Supporting Documentation**

## D.1 Full Technical Specifications for Edge Collision Detection Unit

Element	Requirement	Description/Justification
<b>Performance</b>		
Latency ( $\mu$ seconds/edge)	0.9	3 times faster than benchmark CPU latency.
Throughput (edges/second)	1,111,111	follows from latency.
<b>Area</b>		
FPGA Area	274,080 LUTs	Maximum number of LUTs on a Kintex-7 Low Voltage FPGA
<b>Interface</b>		
Constraints		
Length $\epsilon$	4	$\epsilon$ defines the max edge length. The space being checked and the output sequence has the dimensions $\epsilon \times \epsilon \times \epsilon$ . 4 was chosen after determining what was feasible for given area.
Inputs		
Edge $e$	$\{(x_1, y_1, z_1), (x_2, y_2, z_2)\}$	An Edge $e$ defined for a 3D configuration space by two points $\{p1, p2\}$ , each defined by a set of 3D coordinates $\{x, y, z\}$ .
Control Inputs	<code>clk, rst, start</code>	The functional unit must have ports for control signals: clock, reset, start. These are required for adding the unit to a processor.
Outputs		
Return Value	$\epsilon^3$ bit sequence	Grids are represented by their index in the sequence. 1 if collides with grid at that index, 0 otherwise.
Control Outputs	<code>done, idle, ready</code>	Output ports for control signals: idle, done, ready. These are required for adding the unit to a processor. These ouput signals are part of the “handshake” interface protocol.

Table D.1: Full Technical Specifications for Edge Collision Detection Unit

## D.2 IEEE Standard for Floating-Point Arithmetic

IEEE Standard for Floating-Point Arithmetic

## D.3 Mapping HoneyBee's Output Sequence to a Grid-Map

Mapping HoneyBee's Output Sequence to a Grid-Map

## D.4 HoneyBee Handshake Control Protocol

Port	Description
<code>start</code>	This signal controls the block execution and must be asserted to logic 1 for the design to begin operation. It should be held at logic 1 until the associated output handshake <code>ready</code> is asserted. When <code>ready</code> goes high, the decision can be made on whether to keep <code>start</code> asserted and perform another transaction or set <code>start</code> to logic 0 and allow the design to halt at the end of the current transaction. If <code>start</code> is asserted low before <code>ready</code> is high, the design might not have read all input ports and might stall operation on the next input read.
<code>ready</code>	This output signal indicates when the design is ready for new inputs. The <code>ready</code> signal is set to logic 1 when the design is ready to accept new inputs, indicating that all input reads for this transaction have been completed. If the design has no pipelined operations, new reads are not performed until the next transaction starts. This signal is used to make a decision on when to apply new values to the inputs ports and whether to start a new transaction should using the <code>start</code> input signal. If the <code>start</code> signal is not asserted high, this signal goes low when the design completes all operations in the current transaction.
<code>done</code>	This signal indicates when the design has completed all operations in the current transaction. A logic 1 on this output indicates the design has completed all operations in this transaction. Because this is the end of the transaction, a logic 1 on this signal also indicates the data on the <code>return</code> port is valid. Not all functions have a function return argument and hence not all RTL designs have an <code>return</code> port.
<code>idle</code>	This signal indicates if the design is operating or idle (no operation). The idle state is indicated by logic 1 on this output port. This signal is asserted low once the design starts operating. This signal is asserted high when the design completes operation and no further operations are performed.

Table D.2: Description of the ports associated with the handshake protocol for HoneyBee. Adapted from Vivado HLS User Guide[22]

## D.5 HoneyBee Interface Synthesis Report

<b>RTL Ports</b>	<b>Direction</b>	<b>Bits</b>	<b>Protocol</b>	<b>C Type</b>
ap_clk	in	1	ap_ctrl_hs	return value
ap_rst	in	1	ap_ctrl_hs	return value
ap_start	in	1	ap_ctrl_hs	return value
ap_done	out	1	ap_ctrl_hs	return value
ap_idle	out	1	ap_ctrl_hs	return value
ap_ready	out	1	ap_ctrl_hs	return value
ap_return	out	64	ap_ctrl_hs	return value
edge_p1_x	in	32	ap_none	scalar
edge_p1_y	in	32	ap_none	scalar
edge_p1_z	in	32	ap_none	scalar
edge_p2_x	in	32	ap_none	scalar
edge_p2_y	in	32	ap_none	scalar
edge_p2_z	in	32	ap_none	scalar

Table D.3: **HoneyBee Interface Synthesis Report** for  $\epsilon = 4$ . Results taken from Vivado HLS synthesis report.

## D.6 HoneyBee Timing Reports

HoneyBee Timing Reports

## D.7 HoneyBee-B Variants

HoneyBee-B Variants

Make all reference to "Drone" uniform to "UAV" (this will require chaniging the "a" to "an" before each occurence - wait actually, do I?.) Also maybe I should clarify this to rotary wing UAVs.

Spell check entire doc

Make all figure headings bold with subtitles.

# Todo list

<input type="checkbox"/> Fix Cover Page Formatting . . . . .	i
<input type="checkbox"/> Rewrite Abstract . . . . .	i
<input type="checkbox"/> Define goal . . . . .	1
<input type="checkbox"/> cite . . . . .	1
<input type="checkbox"/> cite . . . . .	2
<input type="checkbox"/> Discuss Moore's law and denard scaling . . . . .	3
<input type="checkbox"/> Improve Problem Statement . . . . .	4
<input type="checkbox"/> Revise End User . . . . .	4
<input type="checkbox"/> Project Specifications . . . . .	9
<input type="checkbox"/> Summary of Results . . . . .	10
<input type="checkbox"/> Update once I have properly defined goals and objectives . . . . .	11
<input type="checkbox"/> System Diagram Here . . . . .	19
<input type="checkbox"/> Appendix Reference? . . . . .	28
Figure: HoneyBee in a Processor . . . . .	33
<input type="checkbox"/> Talk about determining honeybee output . . . . .	45
<input type="checkbox"/> Motion Planning Extension . . . . .	47
<input type="checkbox"/> Description of Baseline Philosophy V core . . . . .	47
<input type="checkbox"/> Display bigger version of processor. . . . .	47
<input type="checkbox"/> Process of implementing honeybee into PhilV. . . . .	49
<input type="checkbox"/> Comparative Performance Analysis of baseline and extended PhilV Core . . . . .	49
<input type="checkbox"/> Discussion of Results . . . . .	50
<input type="checkbox"/> Evaluation of Success . . . . .	50
<input type="checkbox"/> Future Work . . . . .	50
<input type="checkbox"/> Budget . . . . .	58
<input type="checkbox"/> IEEE Standard for Floating-Point Arithmetic . . . . .	70
<input type="checkbox"/> Mapping HoneyBee's Output Sequence to a Grid-Map . . . . .	70
<input type="checkbox"/> HoneyBee Timing Reports . . . . .	72
<input type="checkbox"/> HoneyBee-B Variants . . . . .	72
<input type="checkbox"/> Make all reference to "Drone" uniform to "UAV" (this will require chaniging the "a" to "an" before each occurence - wait actually, do I?.) Also maybe I should clarify this to rotary wing UAVs. . . . .	73

<input type="checkbox"/>	Spell check entire doc . . . . .	73
<input type="checkbox"/>	Make all figure headings bold with subtitles. . . . .	73